Pleistocene paleoenvironmental evolution at continental middle latitude inferred from carbon and oxygen stable isotope analysis of ostracodes from the Guadix-Baza Basin (Granada, SE Spain)

José E. Ortiz [a,*], Trinidad Torres [a], Antonio Delgado [b], Emilio Reyes [b], Juan F. Llamas [a], Vicente Soler [c], Jorge Raya [b]

[a] *Laboratory of Biomolecular Stratigraphy, Madrid School of Mines, C/Ríos Rosas 21, 28003 Madrid, Spain*
[b] *Estación Experimental del Zaidín" (CSIC), C/Profesor Albareda 1, 18008, Granada, Spain*
[c] *Instituto de Agrobiología y Productos Naturales (CSIC), Avda Astrofísico Fco, Sánchez 3, 38206 La Laguna, Tenerife, Spain*

Abstract

A representative paleoenvironmental reconstruction of continental middle latitude from ca. 2 my to the upper part of Middle Pleistocene (279±77 ky) was obtained from the carbon and oxygen stable isotopes analyzed in ostracode shells (*Cyprideis torosa*) recovered in the Guadix-Baza Basin (SE Spain), an intramontaneous closed depression filled by alluvial and lacustrine sediments. This study was performed along a 356-m-thick composite section, dated previously by paleomagnetism and the amino acid racemization method. $\delta^{13}C$ and $\delta^{18}O$ profiles reflected changes in temperature, the evaporation/infill ratio in the water bodies and the amount of rain. $\delta^{13}C$ is also affected by changes in plant biomass: periods with high $\delta^{13}C$ and $\delta^{18}O$ values are associated with warm and dry regimes, and with less vegetation, which, in some cases, coincide with the development of displacive gypsum crystals, whereas low $\delta^{13}C$ and $\delta^{18}O$ values correlate with cold and humid episodes, which cause more vegetation biomass and, therefore, increasing the input of isotopically light carbon. Intermediate $\delta^{18}O$ values are linked to temperate dry or humid episodes when they coincide with high or low $\delta^{13}C$ values, respectively. 86 paleoclimatic events were distinguished in the Pleistocene record from the $\delta^{13}C$ and $\delta^{18}O$ profiles. From both the statistical analysis of the geochemical data and the geological observations, four Cold and Humid Long Periods (low $\delta^{18}O$) and four Warm and Dry Long Periods (high $\delta^{18}O$) were defined. This differs with respect to the paleoclimatological behavior established for the Northern Hemisphere where during cold periods (glacial), no water was available while permafrost conditions persisted, whereas in warm episodes (interglacial), higher precipitation rates occurred. Good correspondences between the Guadix-Baza Basin paleoclimatic record and a marine oxygen-isotope sequence, two continental cores and other long Mediterranean paleoenvironmental records (pollen sequences from Israel) were found, which suggested that climate changes in the Guadix-Baza Basin were in tune with global climatic changes.

1. Introduction

Long paleoenvironmental continental series ranging some hundreds of thousand years are rare for the Pleistocene (Table 1): those covering less than 100 ky B.P. are more common. Most of them rely on pollen data and only a few show stable isotope data. Likewise, three of these latter ones are located in high-latitude areas with temperatures lower than −20 °C even in summer (GRIP, Vostok and EPICA; Dansgaard et al., 1993; Petit et al., 1999; EPICA group, 2004). The Devil's hole core, with $\delta^{18}O$ and $\delta^{13}C$ profiles, ranges up to 570 ky (Winograd et al., 1992; Coplen et al., 1994). The Guadix-Baza Basin (Granada, Spain), located in middle latitude (37°N), appears to be a unique area, i.e., almost "continuous" continental sedimentation took place from the Pliocene until ca. 280 ky BP (cf. Torres et al., 2003a,b). The geographical position of the Iberian Peninsula, in the Mediterranean realm and between Northern Europe and Africa, makes it particularly interesting for the study of the paleoclimatic evolution of continental middle latitude during the Pleistocene. The influence of both Mediterranean and North Atlantic dynamics on its temperature and precipitation caused singular climatic effects in Mediterranean Iberia (Millán et al., 2005), after the Last Glacial Maximum at least (cf. Pons and Reille, 1988; Valero-Garcés et al., 1998, 2000).

Paleoenvironmental and paleoclimatological reconstructions can be achieved by the aid of a number of analytical techniques. Of these, carbon and oxygen stable isotope analysis of biogenic carbonates has been satisfactorily used in ostracode valves (Durazzi, 1977; Lister, 1988; Niessen and Kelts, 1989; Lister et al., 1991; Eyles and Schwarcz, 1991; Schwarcz and Eyles, 1991; Rogers et al., 1992; Dean and Stuiver, 1993; Boomer, 1993; Anadón et al., 1994; Dettman et al., 1995; Holmes et al., 1997; Schwalb et al., 1999; Ricketts et al., 2001; Schwalb and Dean, 2002).

Table 1
Compilation of the largest known paleoenvironmental continental series

Name	Age (ky B.P.)	Environment	Main paleoenvironmental proxies	References
Lake Baikal, Siberia (Russia)	0–12,000	Tectonic lake	Pollen, inorganic and organic geochemistry, paleobiology	Kashiwaya et al. (2003)
Hula Basin, Israel	0–3500	Tectonic lake	Pollen	Horowitz (1987, 1989, 2001)
Jordan Rift Valley, Israel	0–3500	Tectonic lake	Pollen	Horowitz (1987, 2001)
Funza I, Colombia	30–1450	Tectonic lake	Pollen	Hooghiemstra et al. (1993)
Padul Basin, Spain	4.5–1000	Peat bog-lake	Pollen, organic geochemistry	Menéndez Amor and Florschütz (1964), Florschütz et al. (1971), Ortiz et al. (2004b)
Dome C, Antarctica	0–900	Ice	δD, CO_2, CH_4, dust, dielectric profile, conductivity	EPICA group (2004)
Owens Lake, USA	0–800	Tectonic lake	Mineralogy, inorganic geochemistry, pollen, paleobiology	Smith and Bischoff (1997)
Tenaghi Philippon, Greece	0–700	Tectonic lake	Pollen	Wijmstra (1969), Wijmstra and Smit (1976), Tzedakis et al. (2003)
Devil's Hole, Nevada, USA	0–570	Karstic (speleothem)	$\delta^{18}O$, $\delta^{13}C$ calcite	Coplen et al. (1994), Winograd et al. (1992, 1997)
Kopais Basin, Greece	0–500	Lake	Pollen	Okuda et al. (2001)
Ioannina Basin, Greece	0–430	Tectonic lake	Pollen	Tzedakis (1993, 1994)
Velay (Bouchet+Praclaux), France	0–430	Maar lakes	Pollen	Reille and de Beaulieu (1990), de Beaulieu and Reille (1992b)
Vostok, East Antarctica	0–420	Ice	δD, $\delta^{18}O$ ice	Jouzel et al. (1993), Petit et al. (1999)
Valle de Castiglione, Italy	0–250	Maar lake	Pollen, $\delta^{18}O$ and $\delta^{13}C$ molluscs	Follieri et al. (1988), Zanchetta et al. (1999)
GRIP Summit, Greenland	0–250	Ice	$\delta^{18}O$ ice	Dansgaard et al. (1993)
Taylor Dome, Antarctica	0–230	Ice	δD, $\delta^{18}O$ ice	Steig et al. (2000), Grootes et al. (2001)
Lynch's crater, Australia	0–190	Volcanic lake	Pollen	Kershaw (1986)
Salar de Uyuni, Bolivia	0–170	Salt flat	Diatoms; $\delta^{18}O$	Fritz et al. (2003)
Les Echets, France	0–140	Peat bog	Pollen	de Beaulieu and Reille (1984)
La Grande Pile, France	0–140	Peat bog	Pollen	Woillard (1978), de Beaulieu and Reille (1992a)

Ostracodes are micro-crustaceans with laterally compressed body and enclosed in a carapace consisting of two dorsally articulated valves. The carapace consists of low-magnesium calcite (which makes it resistant to diagenetic processes to some extent), though some other ions are present as trace elements (Sohn, 1958; Cadot and Kaesler, 1977; Bordegat, 1979, 1985). Calcification takes place very quickly, from a few hours (Turpen and Angell, 1971) to some days (Chivas et al., 1983; Roca and Wansard, 1997), in geochemical equilibrium with the water in which it is formed. In addition, the composition of the valves does not change once they are constructed.

In the Guadix-Baza Basin, a previous study reflected the abundance of ostracodes in several stratigraphic sections (Anadón et al., 1986). Afterwards, a 356-m-long composite section (cf. Ortiz, 2000; Torres et al., 2003a; Ortiz et al., 2004a) was obtained, containing a very rich record of ostracodes, and therefore, the isotopic study of their valves will provide climatic information for that region from ca. 2 my to 300 ky, expanding the knowledge obtained from ice cores, speleothems, tufa deposits and lacustrine sediments. Oxygen and carbon stable isotope analyses were performed on the valves of the ostracode *Cyprideis torosa* (Jones).

The aim of this paper is to establish a paleoclimatic series in a continental record of continental middle latitude, covering most of the Quaternary. The study of isotope ratios ($^{18}O/^{16}O$ and $^{13}C/^{12}C$) provided information about the paleohydrological evolution and development of the vegetation cover from ca. 2 my to 280 ky.

2. Geographical and geological setting

The Guadix-Baza Basin is a "basin and range"-like endorrheic depression covering ca. 4500 km^2 in the central part of the Betic Range (Fig. 1) and on the Northeast edge of Granada Province (Andalusia, Southeast Spain). It has an irregular shape, with its maximum length oriented SW–NE and is 900–1000 m a.s.l. The climate today is typically Mediterranean with a strong continental influence: winters are cold and dry whereas summers are extremely hot, with daily maximum temperatures reaching over 40 °C. Average annual rainfall ranges from 300 to 350 mm $year^{-1}$, evapotranspiration is 700–900 mm $year^{-1}$, and mean annual temperature is 12–15 °C (Worldwide Bioclimatic Classification System Index). This semi-arid climate favors the development of a badland landscape, mainly covered by steppe plants. Large trees are only found along the scarce rivers that run through the basin. Along the basin, there are also springs with outflows characterized by their brackish, either carbonated or sulfated, waters.

The origin of the Guadix-Baza Basin is related to the Alpine Orogeny (Soria, 1993), which affected Mesozoic and Cenozoic rocks within the region. The bedrock is composed mainly of Mesozoic limestones, dolostones, marls and gypsum, and Neogene sediments of marine origin. Later, during the Upper Tortonian, the sedimentary conditions changed to a continental regime (Vera, 1970; Guerra Merchán, 1990; Soria, 1996).

A detailed description of the stratigraphy of the Guadix-Baza Basin can be found in Torres et al. (2003a). In brief, the basin can be understood as a

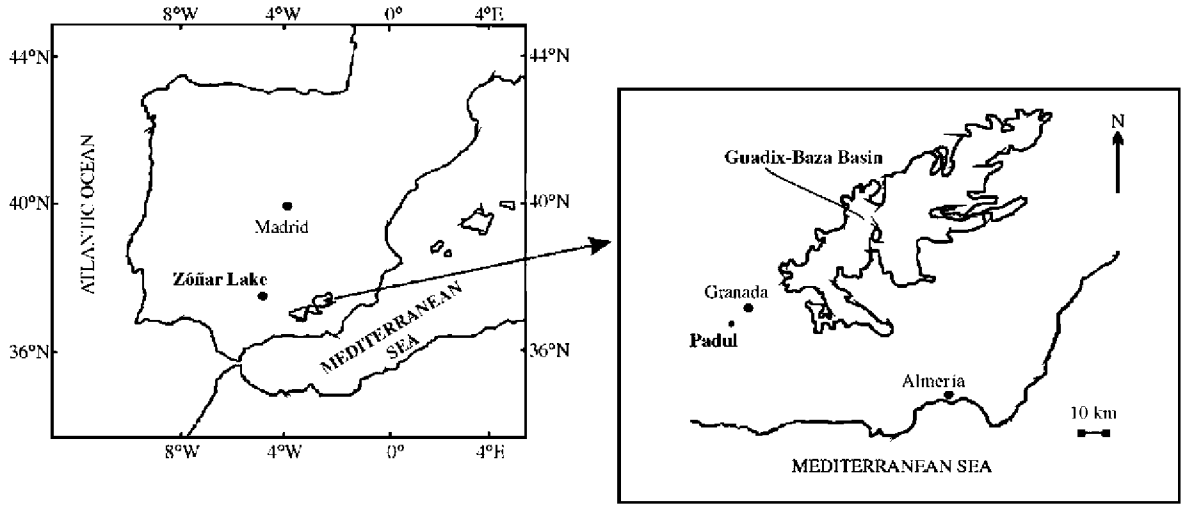

Fig. 1. Geographical location of the Guadix-Baza Basin. The position of the Zóñar lake is also shown.

centripetal depositional model (Fig. 2), i.e., coarse-grained alluvial fans at the foot of mountain ranges, which gradually pass into a system of channels flowing out to a central system of relatively shallow saline lakes, distributed in a mosaic pattern and with sedimentation of gypsiferous lutites, gypsiferous sands, gypsum and, sometimes, thin lutite beds with displacive gypsum crystals (Torres et al., 2003a).

At the end of Middle Pleistocene, erosive processes began, and the current fluvial system was established (Vera, 1970; Peña, 1985; Ortiz et al., 2000), producing the typical badlands landscape that can be seen today. Likewise, the basin drainage changed completely, from endorheic to exorheic towards the Atlantic Ocean via the River Guadalquivir (Viseras and Fernández, 1992; Calvache and Viseras, 1997).

Three main depositional settings (facies) are distinguished: (1) upper alluvial fan massive gravels and lens-shaped channeled sands and gravels; (2) sand playa deposits and mud flat playa (red lutites); and (3) lacustrine sands and grey lacustrine gypsiferous lutites and sands, carbonate and gypsum beds (Torres et al., 2003a).

Lacustrine events did not usually fill up the whole basin, which highlights the existence of a "microenvironmental mosaic" with independent and shallow-water bodies that were then connected during pluvial stages. Some of them would have been fed directly by alluvial fans' distribution channels and others could be linked to saline or brackish springs. This sedimentation pattern with a distinctive lacustrine expansion event (Orce Limestone Horizon) continued until the upper part of Middle Pleistocene (Ortiz et al., 2000; Torres et al., 2003a).

The composite section established for the Pleistocene paleoenvironmental study in the East domain of the Guadix-Baza Basin is 356 m thick. It is composed of two sub-sections: Cortes de Baza (UTM_{bottom}: 201679; UTM_{top}: 223670) and Norte de Orce (UTM_{bottom}: 423770; UTM_{top}: 337807) sections. Its chronostratigraphy, reported in Ortiz (2000) and Ortiz et al. (2004a), was obtained by paleomagnetism and the amino acid racemization dating method (Fig. 3). According to magnetostratigraphic studies of the Basin (Oms et al., 1994; Ortiz, 2000), supported by paleontological data (Agustí, 1986), three important paleomagnetic events took place: the end of the Olduvai chron (ca. 1.77 My), the Matuyama/Brunhes boundary (ca. 780 ky) and a short reverse polarity event corresponding to either Emperor or Lake Biwa III excursions, dated at ca. 419 ky or ca. 412 ky (Cande and Kent, 1995), respectively. The top of the section was dated by amino acid racemization at 279±77 ky (Ortiz et al., 2004a). Detailed lithological and stratigraphical descriptions of the section can be found elsewhere (Ortiz, 2000; Torres et al., 2003a).

3. Materials and methods

A total of 726 samples were taken approximately at 40–50-cm intervals along the composite section. Samples were sieved (at 2.5 cm and 250 μm) and studied under a binocular microscope to select the ostracodes. We chose the *C. torosa* species because its valves are abundant and continuously distributed along the section. Another reason for selecting it was that it can live in waters with a wide range of salinity, varying from 0.5‰ to 60‰ (De Deckker, 1981), although according to Carbonnel (1983), it can reaches up to 140‰. This means that the valves reflect very different hydrogeochemical conditions, and so paleoenvironmental evolution throughout the section time span can be obtained from them.

For stable isotope analyses, 30–50 *C. torosa* valves were selected, although there were some samples with fewer, in some cases 4, ostracodes. 424 samples contained a sufficient number of *C. torosa* valves to be analysed. We avoided the use of juveniles, as suggested by Heaton et al. (1995), and selected either left or right valves of males and females because there were no significant differences between the valves or between sexes of the same species (Heaton et al., 1995).

The selected valves of *C. torosa* were sonicated and cleaned under running milli-Q water and dried at room temperature. Before the isotopic analysis, the samples were heated at 400 °C under a nitrogen atmosphere for 1 h to remove the remaining organic matter. Carbon dioxide was evolved from the calcite using 100% phosphoric acid for 30 min in a thermostatic bath at 80 °C (McCrea, 1950; Swart et al., 1991). A Pyrex microline was used for gas purification. The carbon and oxygen stable isotope analyses were conducted in a Finnigan MAT 251 mass spectrometer at the Estación Experimental del Zaidín (CSIC, Granada). The isotope results are reported in the standard delta (δ) notation in parts per thousand (‰) relative to the international V-PDB standard (Gonfiantini, 1981). All the samples were compared to a reference carbon dioxide obtained from a calcite standard (internal and international standard) prepared at the same time. The experimental error for calcite ($\delta^{13}C$ and $\delta^{18}O$) was less than ±0.1%. Carrara and EEZ-1 were used as internal standards that had been previously compared with the international standards NBS-18 and NBS-19.

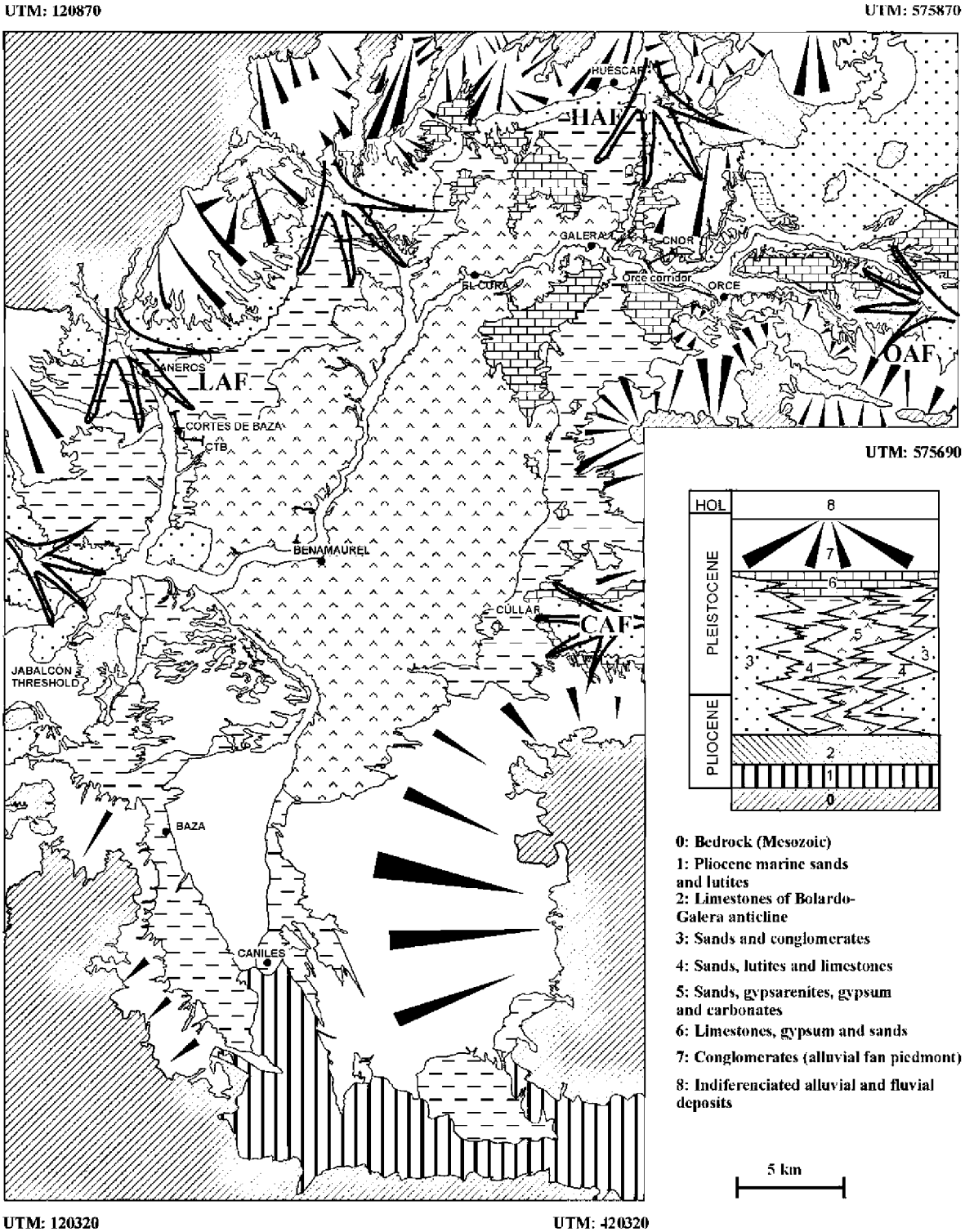

Fig. 2. Simplified geological map of the east domain of the Guadix-Baza Basin. LAF=Laneros Alluvial Fan, OAF=Orce Alluvial Fan, HAF=Huéscar Alluvial Fan, CAF=Cúllar Alluvial Fan. CTB: Cortes de Baza stratigraphic section; CNOR: Norte de Orce stratigraphic section.

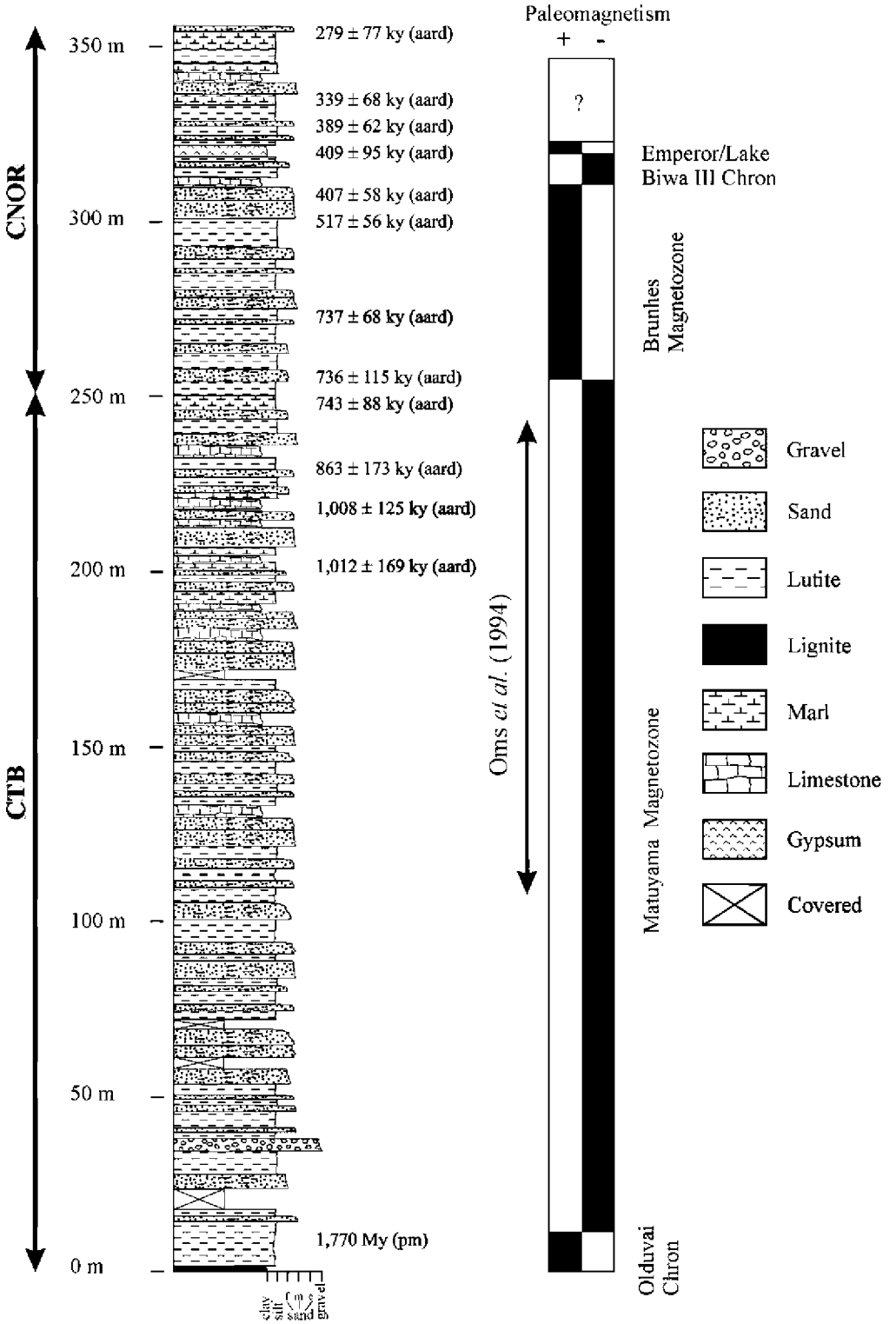

Fig. 3. Chronostratigraphy of the Guadix-Baza Basin composite stratigraphic section, using the amino acid racemization method and paleomagnetism. Paleomagnetism results are based on Ortiz (2000) and Oms et al. (1994), modified from Ortiz et al. (2004a).

4. Results

The $\delta^{13}C$ values in *C. torosa* valves run between −9.68‰ and −2.0‰ (V-PDB) and the $\delta^{18}O$ values range from −11.08‰ to +4.9‰ (V-PDB). However, the most frequent values range between −2.5‰ and −6‰ for $\delta^{13}C$ and between −0.5‰ and −3.5‰ for $\delta^{18}O$ (Fig. 4a and b). Former isotope studies of the basin, which were markedly local in character, appear in Bonadonna and Leone (1989) and Anadón et al. (1994).

The well-defined continuous trends indicate the absence of diagenetic processes, which should be reflected in homogenization of the isotope signal. The calcitic composition of the ostracode valves, its aridity and the absence of cementation were important factors in the preservation of the isotope signal.

5. Discussion

The $^{18}O/^{16}O$ ratio in authigenic carbonates and, therefore, in ostracode valves, depends on both the $^{18}O/^{16}O$ ratio of the host water in which they were formed and temperature. However, as temperature falls, the ^{18}O content of rainwater decreases (Dansgaard, 1964; Rozanski et al., 1993; Longinelli and Selmo, 2003), while in the calcite that forms in equilibrium with

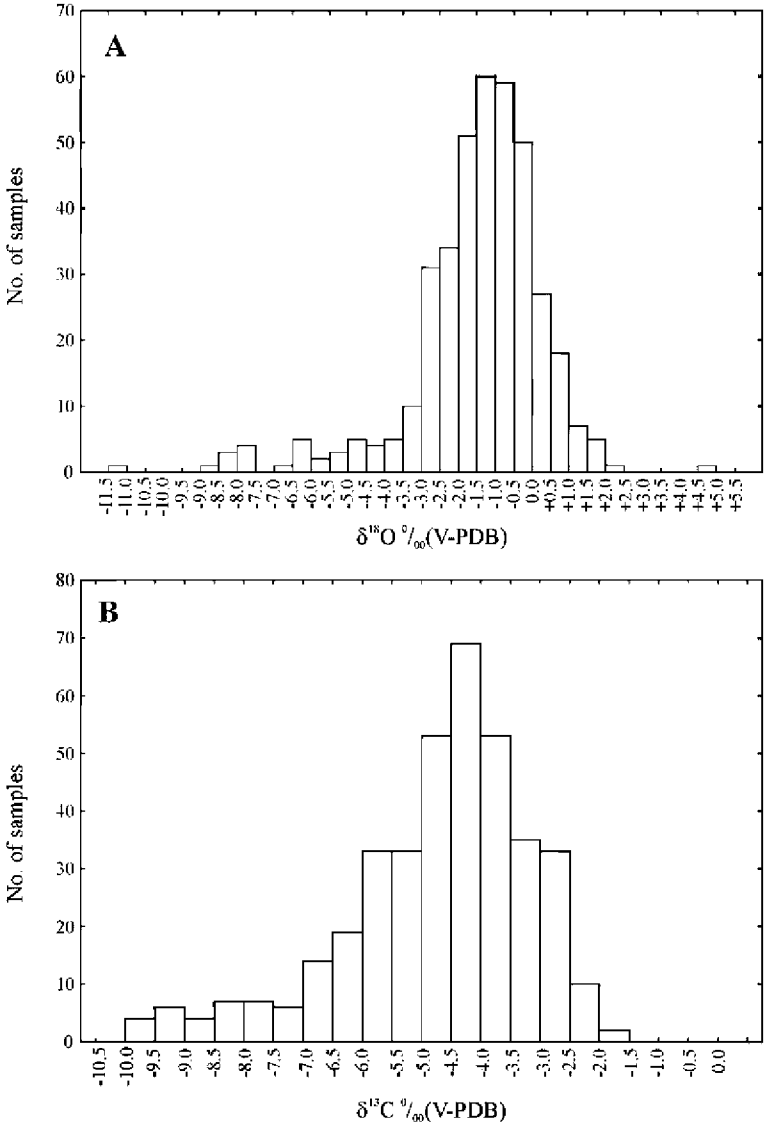

Fig. 4. Histogram of $\delta^{18}O$‰ (V-PDB) (A) and $\delta^{13}C$‰ (V-PDB) (B) values obtained in ostracode shells (*Cyprideis torosa*) from the Guadix-Baza Basin composite section.

rainwater, the opposite occurs. These two phenomena overlap, thereby complicating the task of a simple relationship between temperature and the isotope composition of the calcite (Delgado, 1994; Delgado and Reyes, 2001). The thermo-dependence fractionation factor (α) for oxygen during calcite precipitation is 0.24‰ per degree centigrade (Craig, 1965; O'Neil et al., 1969; Kim and O'Neil, 1987). However, a 1 °C temperature decrease lowers rainwater $\delta^{18}O$ values by 0.69‰ (Dansgaard, 1964). As a net result, the effect of rainwater is more important than temperature. However, the value provided by Dansgaard (1964) depends on latitude, "averaging perhaps 0.4–0.5‰ in temperate regions" according to Broecker (1992), and averaging 0.35–0.40‰ for the Mediterranean area (Hauser et al., 1980; Delgado et al., 1991). In the case of organisms with carbonate valves, vital effects (fractionation produced by the calcification) should be taken also into account.

Despite the relatively wide range of variation in $\delta^{18}O$ values, the histogram of Fig. 4 reveals that most of them are grouped between +0.5‰ and −3.5‰ (V-PDB). Based on this distribution range and on the estimated vital temperature range (8–30 °C) of *C. torosa* ostracodes (Carbonnel, 1983; Wansard et al., 1998; Mezquita et al., 2000), the theoretical $\delta^{18}O_{water}$ values (V-SMOW) expected should range between +3.5‰ and −4.9‰ (Fig. 5). However, given the most common temperature range (15–25 °C) at which *C. torosa* flourishes (Planas, 1973; Heip, 1976), the expected range of $\delta^{18}O_{water}$ values (V-SMOW) should be from +2.50‰ to −3.50‰.

We will now take into account the $\delta^{18}O$-enrichment in ostracode valves as a result of vital effects for the calculation of the expected $\delta^{18}O_{water}$ values (V-SMOW) between 15 and 25 °C. According to von Grafenstein et al. (1992, 1999) and Keatings et al. (2002), the maximum offset is around +2.5‰, although some authors found that ostracode valves were enriched by as little as 0.73, while most of them, depending on the species, are by ca. +1‰ (Xia et al., 1997; von Grafenstein et al., 1999). However, recently, Chivas et al. (2002) showed that the $\delta^{18}O$ vital offset of ostracode valves is reduced at low temperatures, being only +0.3‰ for *Australocypris robusta* at 12 °C, while at higher temperatures, it is +0.7‰, although the influence of pH cannot be totally discarded. Similarly, von Grafenstein et al. (1999) found no significant $\delta^{18}O$ vital offsets for different ostracode species from lakes with temperatures as low as 3.5 °C. In any case, although it seems that there are different vital offsets depending on temperature, we will use the maximum value (+2.5‰) for the temperature range (15–25 °C) considered, being the expected $\delta^{18}O_{water}$ values (V-SMOW) between +0.2‰ and −5.8‰ (V-SMOW).

In all cases, these ranges of $\delta^{18}O$ values are a bit higher than those at present in waters from reservoirs located close to the study area and the average $\delta^{18}O$ values of present rainwater in Granada (Fig. 5), indicating that other factors related to climate evolution affected the $\delta^{18}O$ signal measured in the ostracode valves of the Guadix-Baza Basin.

The $\delta^{13}C$ signal from ostracodes is mainly influenced by the $\delta^{13}C$ of the dissolved inorganic carbon (DIC), which, in turn, is mainly controlled by vegetation (inputs of DIC from terrestrial respiration), lake area, pH, alkalinity, residence time or productivity (cf. Boomer, 1993; Palacios-Fest et al., 1993; Anadón et al., 1994; Holmes et al., 1997; Schwalb et al., 1999; von Grafenstein et al., 1999; Bade et al., 2004). These factors can be linked to climatic conditions, i.e., evaporative processes together with arid conditions should produce an increase in $\delta^{13}C_{water}$ due to degasification processes and isotopic exchange between atmospheric CO_2 and $CO_{2(aq)}$. On the contrary, in semiarid areas, humid periods are characterized by an increasing in the vegetal biomass and respiration. Consequently, input of DIC would give more negative in $\delta^{13}C$. Moreover, changes in climate may modify the vegetation cover (amount and proportion of C3 to C4 plants in the catchment) and, ultimately, the $\delta^{13}C$ derived from the terrestrial respiration that reaches a lake.

The range of $\delta^{13}C$ values in ostracode valves from the Guadix-Baza Basin coincides with the highest $\delta^{13}C$ values of present river DIC and ancient and present-day tufas from nearby areas (Fig. 6). These values are between the theoretical $\delta^{13}C$ expected for calcite precipitated under humid and arid conditions.

The oxygen and carbon isotope ratios of continental carbonates reflect paleohydrological conditions rather than temperature (Gasse et al., 1987; Lister, 1988; Lister et al., 1991; Anadón et al., 1994; Heaton et al., 1995; Holmes et al., 1997, among others). In middle latitudes and, especially, in regimes with a semi-arid climate, there is a clearly marked seasonal effect in the isotopic composition of rainwater, together with the "amount of rain effect", i.e., during cold episodes and when precipitation is high, the isotope composition of rainwater is more negative (Riesenfeld and Chang, 1936; Belatini de, 1959; Fontes et al., 1985; Rozanski et al., 1993; Longinelli and Selmo, 2003). However, during warm periods, which, in the Mediterranean realm, are usually linked to low precipitation rates, surface waters are ^{18}O-enriched due to rainwater

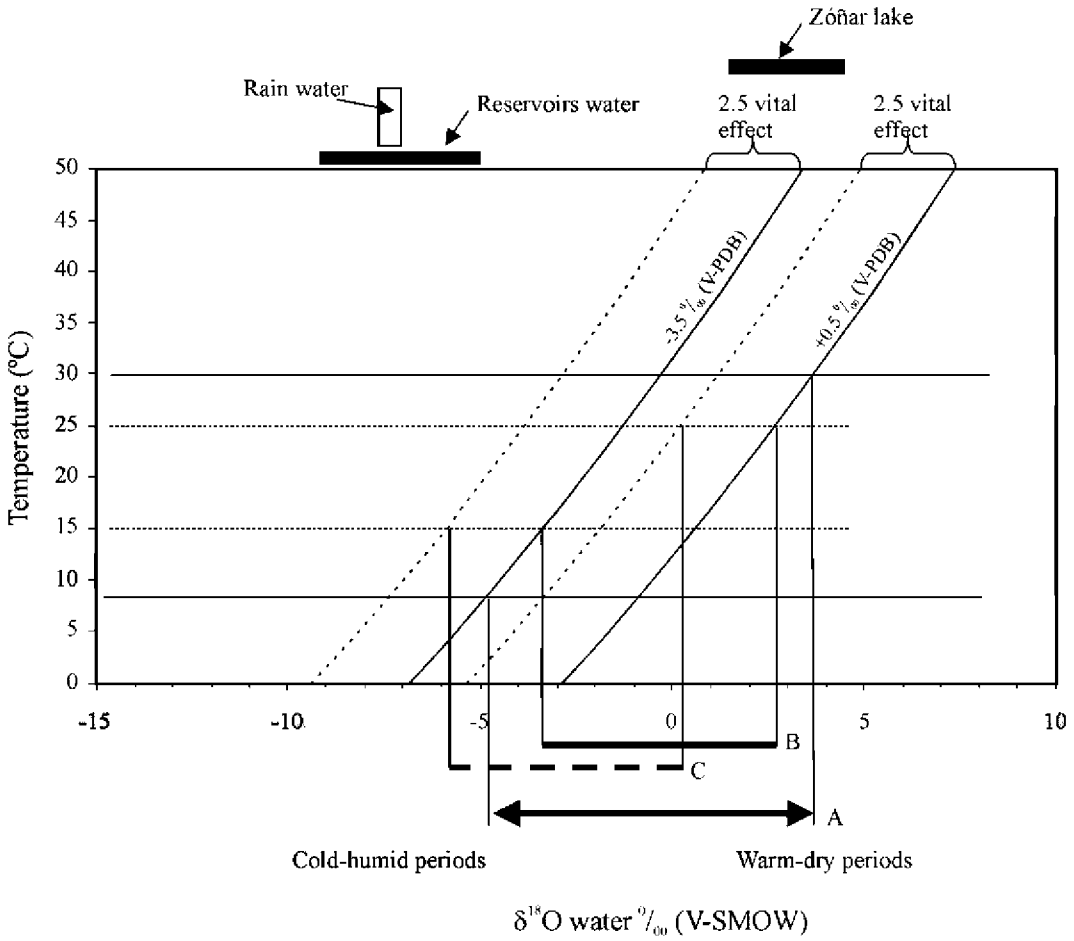

Fig. 5. Diagram showing temperature and $\delta^{18}O‰$ (V-SMOW) values of waters. The curves represent the theoretical temperature of formation of calcite–ostracodes in equilibrium with lake waters. The Kim and O'Neil (1987) calcite–water equation was used for calculation. The vital temperature range (8–30 °C) for *Cyprideis torosa* (Carbonnel, 1983; Wansard et al., 1998; Mezquita et al., 2000) and the most frequent range of isotopic values measured in ostracodes from the Guadix-Baza Basin composite section ($-3.5‰ < \delta^{18}O < +0.5‰$ vs. V-PDB) were used to calculate the isotopic composition of the meteoric waters (line A). To calculate lines B and C, the most common interval of the temperature at which *C. torosa* flourishes (15–25 °C; Planas, 1973; Heip, 1976) was used; and both the absence and presence of vital effects [although it seems that the $\delta^{18}O$-enrichment in ostracode valves as a result of vital effects varies with temperature (Chivas et al., 2002), we used the maximum offset as +2.5‰ (cf. von Grafenstein et al. (1992, 1999) and Keatings et al. (2002)) for the whole temperature range] were considered to calculate the corresponding $\delta^{18}O‰$ (V-SMOW) range. For comparison, present values of rainwater (pondered average) and the range of surface waters from reservoirs located in nearby areas (Cubillas, Canales, Bermejales and Quentar) are plotted.

becoming steadily heavier, and because of the evaporation effect (Gasse et al., 1987; Fontes and Edmunds, 1989). Therefore, high values of $\delta^{18}O$ indicate low (less than 1) precipitation/evaporation (*P/E*) ratios (Lister, 1988; Lister et al., 1991; Holmes et al., 1997).

Ostracode shells with more positive $\delta^{18}O$ values (+0.5 to +4.9‰) indicate, even at a wide range of temperatures (8–30 °C), that their calcification took place in equilibrium with waters with $\delta^{18}O$ values between −1.0‰ and +7.5‰ (V-SMOW) (see Fig. 5 for reference). These values are much higher than the characteristic values of open-system waters from actual reservoirs in this area (−5‰ to −9‰ vs. V-SMOW, Fig. 5), the average $\delta^{18}O$ value of rainwater in Granada (−7.5‰ vs. V-SMOW, Delgado et al., 1991) or characteristic values for middle latitudes (Rozanski et al., 1993). Therefore, these $\delta^{18}O$ values reflect phases with important evaporation. In fact, some endorrheic Iberian Peninsula lakes located in arid or semi-arid areas show positive $\delta^{18}O$ values (higher than +5‰) at the end of the dry seasons (Valero-Garcés et al., 2000). Similarly, in Lake Zóñar (Córdoba, Andalusia), an endorrheic relatively shallow (17 m deep) lake about 140 km northwest of the Guadix-Baza Basin, $\delta^{18}O$

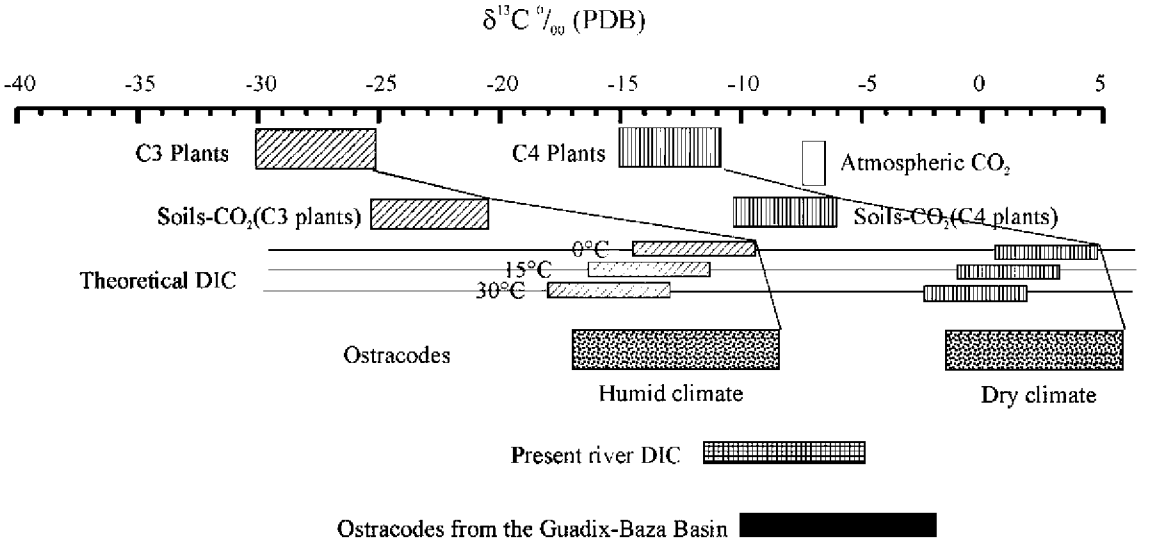

Fig. 6. Graph of the different sources of carbon. Only C3–C4 plants and atmosphere CO_2 are included, since CAMP plants are insignificant in most ecosystems (Deines, 1980; Cerling, 1991). The pre-industrial atmosphere CO_2 with a $\delta^{13}C$ value of −6.5‰ (Friedli et al., 1986) is also shown. The rectangles show the most frequent range of $\delta^{13}C$ values for C3 and C4 plants (Deines, 1980), as well as soil CO_2 for areas dominated by either C3 or C4 plants, and the corresponding $\delta^{13}C$ values of dissolved inorganic carbon (DIC) produced in water bodies. Soil CO_2 is about 4.5‰ heavier than its corresponding plant biomass (C3–C4) (Cerling, 1984, 1991). The isotopic difference between CO_2 and dissolved inorganic carbon (DIC) depends on pH and temperature. This difference is near 0‰ at pH values close to 5, but for pH values between 7.5 and 8, it is relatively independent (Romanek et al., 1992), becoming enriched at 10‰. Consequently, surface water input from light basic areas is enriched in about 14.5‰, while light acid is less enriched. For the theoretical isotopic calculation (DIC and ostracode valve calcites), we took a calcite–bicarbonate enrichment of 1‰ (independent of the temperature) and the calcite–CO_2 equation described by Romanek et al. (1992) for temperatures of 0 °C, 15 °C and 30 °C. Ostracode valve calcite values are represented for humid and arid episodes. For comparison, we added the $\delta^{13}C$ range of present DIC values measured in rivers from this basin and nearby areas and $\delta^{13}C$ values of old and present tufas from the study area.

values are high (+1.5‰ V-SMOW in humid seasons; +4.4‰ V-SMOW in dry seasons; Valero-Garcés et al., 2006). For comparison, the calculated range for $\delta^{18}O_{water}$ in the lacustrine system of the Guadix-Baza Basin in about 1.6my was relatively narrow, indicating that the $\delta^{18}O$ profile obtained was a reflection of major paleoclimatic changes, but not of seasonal variations.

These samples with positive $\delta^{18}O$ values are characterized by relatively high $\delta^{13}C$ values (greater than −4‰), indicating that the calcification of the valves took place in waters with ^{13}C-enriched DIC (Dissolved Inorganic Carbon). Nowadays, the various rivers that feed the Guadix-Baza Basin have $\delta^{13}C_{DIC}$ values ranging between −13‰ and −6‰ (monthly analysis of water samples from 30 rivers and brooks with their catchment areas in the Sierra Nevada; unpublished data) (Fig. 6). This enrichment ^{13}C could be explained by a decrease in the terrestrial biomass and/or evaporation–degasification processes causing increased $\delta^{13}C$ (Talbot, 1990; Mees et al., 1998; Stiller et al., 1985; Schwalb et al., 1999; Valero-Garcés et al., 2000). Likewise, C4 plants, which are characterized by their $\delta^{13}C$ values being about 15‰ higher than C3 plants, are especially adapted to warm areas, where night temperatures do not drop below 8 °C (Teeri and Stowe, 1976), and to semi-arid regions, as their WUE (water-use efficiency) is high (Pate, 2001; Sage, 2004). Thus, when dry periods coincide with temperature increases, which are favorable conditions for the development of C4 land-plants (Cerling, 1984; Sage, 2004), vegetable cover contributes with less negative values to the DIC $\delta^{13}C$ signal (Fig. 6).

In addition, the contribution of atmospheric CO_2 (less negative source) to surface waters is a bit higher during dry episodes, due to the scarce plant cover (less river DIC and DOC inflow). An alternative explanation has to do with the phytoplankton blooms that produce a preferentially active uptake of ^{12}C by lake waters (Spiro et al., 1993). However, these changes linked to productivity occur in a short time (days or weeks) and do not explain general shifts.

Thus, during episodes of higher aridity and temperature, which are associated with (a) higher evaporation rates, (b) a less water input (DIC and DOC), and (c) a less ratio respiration/photosynthesis ratio, an increase in both $\delta^{18}O$ and $\delta^{13}C$ values is linked to evaporation and the increase of the atmospheric CO_2 contribution

(Talbot, 1990; Mees et al., 1998; Stiller et al., 1985; Schwalb et al., 1999). These processes change the water chemistry, by increasing pH and alkalinity, producing a major isotopic exchange and capture of atmospheric CO_2. Increased $\delta^{13}C$ values are also linked to increased plant C4 and/or decreased plant biomass (causing a relative increase in atmospheric CO_2 contribution), typical of semi-arid areas.

The ostracode shells with the most negative $\delta^{18}O$ values (−11.1‰ vs. V-PDB) would have been built in equilibrium with waters with $\delta^{18}O$ values ranging from −13‰ to −8‰ (V-SMOW). However, extremely negative values are relatively scarce (Fig. 4a); the commonest values run from −4 to −9‰ (V-PDB), which are given by waters with $\delta^{18}O$ values between −11‰ and −1‰ (V-SMOW) (see Fig. 5 for reference). These are, in part, lower than the rainwater $\delta^{18}O$ values (−7.5‰ V-SMOW) obtained in Granada and the $\delta^{18}O$ range from the reservoirs in neighboring areas. This may be interpreted as a result of periods of falling temperature (more negative isotopic composition of rainwater), which, in middle latitudes, is normally linked to more precipitation and less evaporation (Fontes and Edmunds, 1989; Rozanski et al., 1993).

These samples (with the lowest $\delta^{18}O$ values: less than −4‰ V-PDB) have marked negative $\delta^{13}C$ values, which are usually associated with more plant cover (humid conditions) and associated more soil respiration, which should be a source of carbon characterized by lower $\delta^{13}C$ values (Cerling, 1984; Sage, 2004), masking the contribution from atmospheric CO_2 (−6.5‰; Friedli et al., 1986). Consequently, samples with more negative $\delta^{18}O$ and $\delta^{13}C$ values should be related to cold and humid episodes (increasing DIC and DOC inputs to the lake: sources of minor ^{13}C), to which C3 plants are better adapted. On the other hand, humid conditions are related with minor pH and alkalinity causing lower $\delta^{13}C$ values in DIC (Romanek et al., 1992; Bade et al., 2004).

Intermediate $\delta^{18}O$ values (−4‰ V-PDB to +0.5‰ V-PDB) should reflect temperate periods: temperate–dry, when they coexist with higher $\delta^{13}C$ values, and temperate–humid, when they occur with lower $\delta^{13}C$ values.

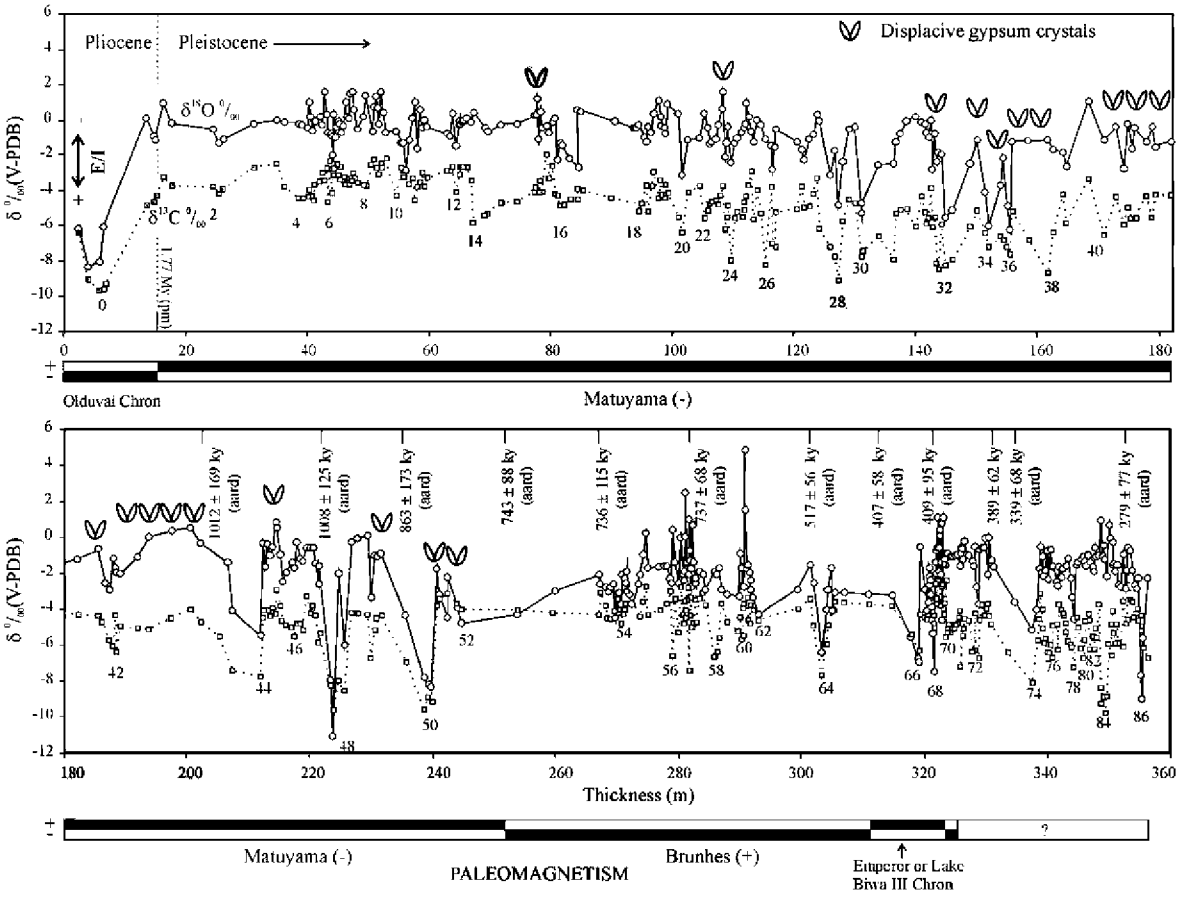

Fig. 7. $\delta^{13}C$ and $\delta^{18}O$ profiles obtained in *Cyprideis torosa* (Jones) ostracodes from Guadix-Baza Basin with the paleoclimatic events identified. The position of displacive gypsum crystals is also shown.

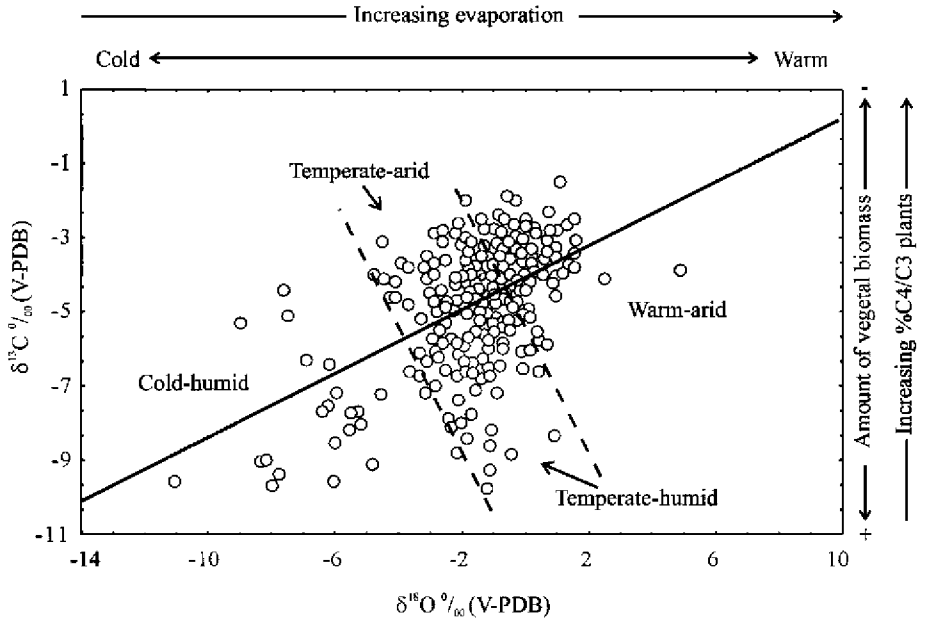

Fig. 8. Regression analysis between the $\delta^{13}C$ and $\delta^{18}O$ values obtained in *Cyprideis torosa* ostracodes from the Guadix-Baza Basin. Four clusters representing paleoenvironmental scenarios are distinguished based on the results of Fig. 9.

We use here the terms cold–humid, warm–dry and temperate as proposed by Horowitz (1989, 2001) for Israel: Pluvial (Wet Mediterranean), with lower temperatures, higher rainfall (moderate rains in winter and summer), and the development of deciduous oak forest; Interpluvial (Dry Mediterranean), with rare precipitation, higher temperatures and steppe vegetation; and Interstadial, like present-day conditions, with a short rainy winter and a dry, hot summer, with evergreen oaks and Mediterranean maquis.

Good covariation between our $\delta^{18}O$ and $\delta^{13}C$ profiles (Fig. 7) is seen. In fact, the correlation coefficient between $\delta^{18}O$ and $\delta^{13}C$ values is significant ($r=0.50$; $p=0.000$; Fig. 8), being higher ($r=0.70$,

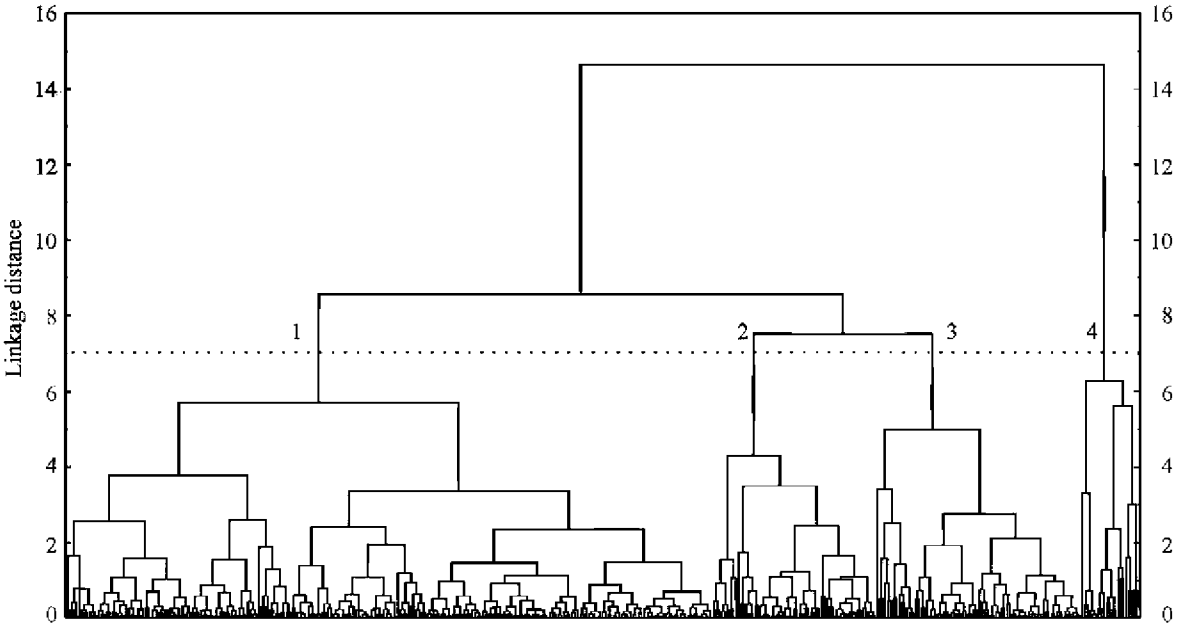

Fig. 9. Dendrogram of the $\delta^{13}C$ and $\delta^{18}O$ values obtained in *Cyprideis torosa* ostracodes from the Guadix-Baza Basin composite section.

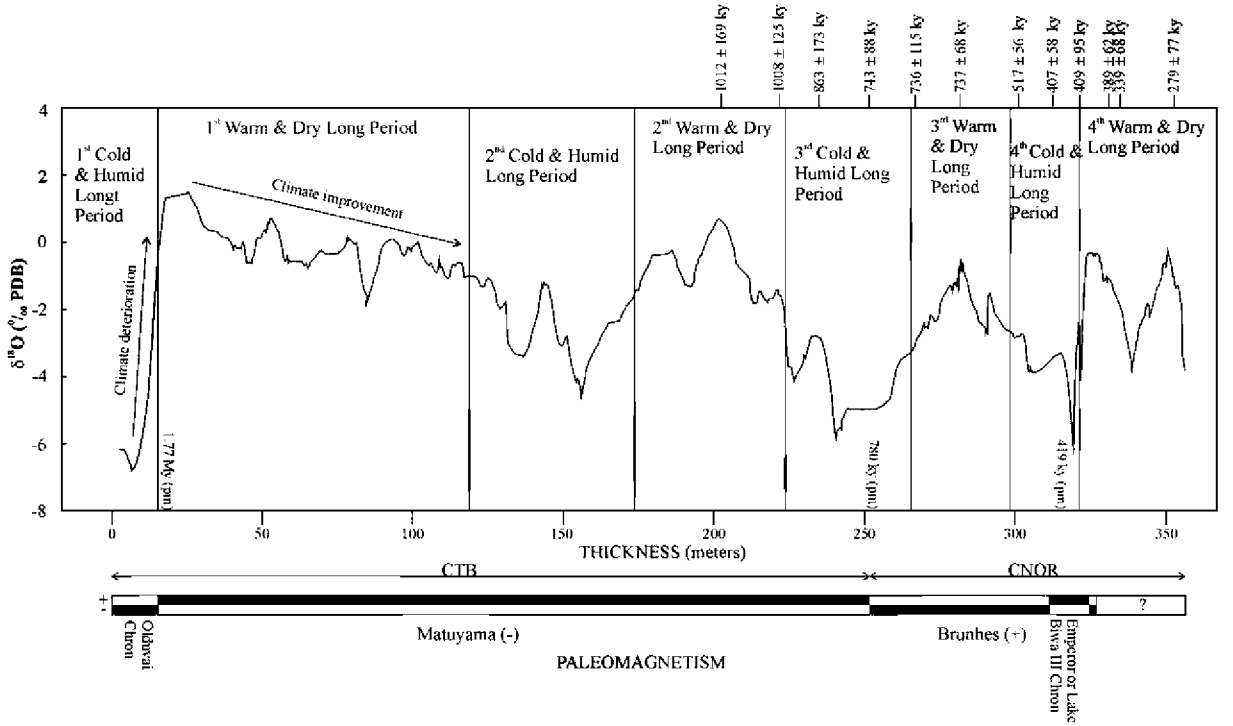

Fig. 10. Smoothed curve of the $\delta^{18}O$ values obtained in *Cyprideis torosa* ostracodes from the Guadix-Baza Basin composite section with the paleoenvironmental periods identified.

$p=0.000$) in the lower 255 m of the section (that corresponds to the Cortes de Baza sub-section-CTB), which confirms the expected covariation of these paleoclimatological proxies in arid or semiarid regions. Likewise, the ostracodes of Guadix-Baza lived in an endorheic basin producing a $\delta^{18}O$–$\delta^{13}C$ correlation coefficient characteristic of carbonates normally precipitated from a closed basin (Talbot, 1990; Li and Ku, 1997).

A cluster analysis (complete linkage and Euclidean distance) was performed on $\delta^{18}O$ and $\delta^{13}C$ values (Fig. 9), in which four groups can be differentiated. Based on these results, these groups can also be distinguished in the linear regression plot between $\delta^{18}O$ and $\delta^{13}C$ and can be matched with different climate scenarios according to the above discussion (see Fig. 8): Group 1, high $\delta^{18}O$ and $\delta^{13}C$ values (warm–dry scenario); Group 2, intermediate $\delta^{18}O$ and high $\delta^{13}C$ values (temperate–dry scenario); Group 3, intermediate $\delta^{18}O$ and low $\delta^{13}C$ values (temperate–humid scenario); Group 4, low $\delta^{18}O$ and $\delta^{13}C$ (cold–humid scenario).

5.1. The Guadix-Baza paleoclimatic events

In the Guadix-Baza Basin composite section, a large number of oscillations were distinguished in the oxygen and carbon isotopic logs and interpreted as paleoclimatic events (Fig. 7). According to Whittaker et al. (1991), "events" are short-lived occurrences, including climatic ones, that leave some trace in the geological record, and which can therefore be used as a basis for correlation. We interpret an isotopic paleoclimatic event when not only a single one, but several, isotopic values show a marked shift in the gradients of both $\delta^{18}O$ and $\delta^{13}C$ values.

Minima in $\delta^{18}O$ and $\delta^{13}C$ values are interpreted as cold and humid episodes, whereas maxima in $\delta^{18}O$ and $\delta^{13}C$ values are linked to warm and dry phases. Intermediate values reflect either temperate–dry or

Table 2
Time range and thickness range of the Guadix-Baza Basin Long Periods defined in the smoothed $\delta^{18}O$ profile (Fig. 10)

Guadix-Baza Basin Long Period	Time range (ky B.P.)	Thickness range (m)
1st Cold and Humid	<1770	<18
1st Warm and Dry	1770–1385	18–120
2nd Cold and Humid	1385–1130	120–175
2nd Warm and Dry	1130–890	175–225
3rd Cold and Humid	890–700	225–270
3rd Warm and Dry	700–575	270–292
4th Cold and Humid	575–410	292–323
4th Warm and Dry	>410	>323

temperate–humid conditions. It should be emphasized that the presence of displacive gypsum crystals, which are formed through evaporative processes ($E \gg P$) in a saline brine, coinciding with some maxima of the $\delta^{18}O$ and $\delta^{13}C$ values, reinforces this explanation (Fig. 7). In fact, according to Rosen (1994), the presence of displacive crystals of evaporites in a sedimentary horizon can be interpreted as a result of high aridity with a markedly negative water balance in the lacustrine system. The presence of displacive gypsum crystals only in the lower part of the composite section (Cortes de Baza sub-section—CTB; Figs. 2 and 6) can be regarded as a reflection of the paleogeographical situation of both sub-sections (CTB and Norte de Orce sub-section—CNOR). The CTB profile is situated near the centre of the Guadix-Baza Basin, whereas CNOR corresponds to a lacustrine margin with visible influence of an alluvial fan, which allowed a more continuous water inflow (Torres et al., 2003a).

Apart from gypsum, no other relation has been found between sediment types and carbon and oxygen composition. There are sand playa and mud flat playa

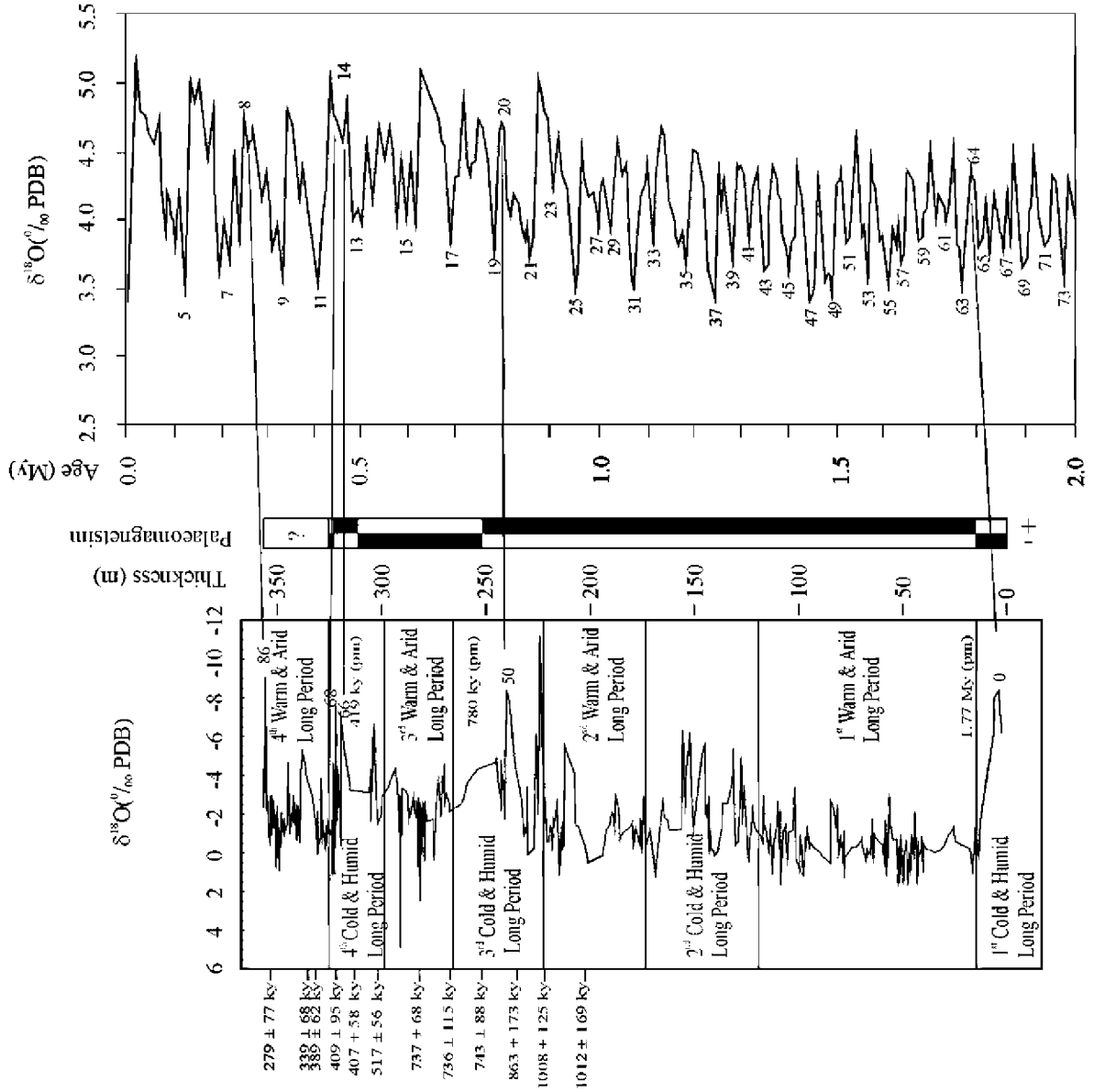

Fig. 11. Correlation between the $\delta^{18}O$ profile of the Guadix-Baza Basin and the marine oxygen isotopic record (Shackleton, 1995). The data of the marine oxygen isotope record derive from the SPECMAP stack for the 0–0.62-my interval and from OPD site 677 for the 0.62–2.0-my interval.

(red lutites) deposits and lacustrine sands and lacustrine gypsiferous lutites, with or without ostracode valves and with different $\delta^{18}O$ and $\delta^{13}C$ values. Furthermore, similar $\delta^{18}O$ and $\delta^{13}C$ values are found in sand and lutite beds.

Owing to the short Pliocene record included in the composite section of the Guadix-Baza Basin, we decided to define only paleoclimatic events from the Quaternary record of the section. Nevertheless, the minima of $\delta^{18}O$ and $\delta^{13}C$ values observed at the top of the Pliocene record were named GB-0 for correlation purposes. Paleoclimatic events (minimum and maximum $\delta^{18}O$ and $\delta^{13}C$ values) were numbered from the Pliocene–Pleistocene boundary to the top of the Guadix-Baza Basin section, from GB-1 to GB-86 (Fig. 7). According to the criteria followed in other paleoclimatic series (e.g., Oxygen Isotope Stages), even numbers correspond to cold events (minimum $\delta^{18}O$ and $\delta^{13}C$ values). The events GB-0, 34, 36, 48, 50, 64, 66, 68 and 86 (lowest $\delta^{18}O$ values) reflect the coldest and most humid conditions, while the warmest and driest events are less clearly defined because of the abundance and homogeneity of samples with high $\delta^{18}O$ values, especially at 20 and 100 m where only slight variations are observed, whereas more pronounced ones are detected in the rest of the sequence. In fact, the cluster analysis (Fig. 9) and the $\delta^{18}O$ vs. $\delta^{13}C$ plot (Fig. 8) show the predominance of samples thought to reflect warm and dry conditions. Nevertheless, the $\delta^{18}O$ maxima correspond to events 5, 7, 9, 23, 39, 45, 57, 61, 69 and 83.

We also performed a smoothing analysis of the $\delta^{18}O$ values with the linear trend method, calculating each smoothed new value from the 5 ones closest to it. Four Cold and Humid Long Periods alternating with four Warm and Dry Long Periods were defined in the smoothed $\delta^{18}O$ profile (Fig. 10), representing long-term episodes of relative climatic stability. The time scales of these periods, based on the available datings and the mean sedimentation rate (4.464 ky/m) of the basin (cf. Ortiz et al., 2004a), are shown in Table 2.

It can be seen in Fig. 10 that climate deterioration (in the Mediterranean realm, warm and dry conditions) is sharp, while transitions to climate improvement (cold and humid conditions) are more gradual.

5.2. Comparison of Guadix-Baza Basin profile with other long paleoenvironmental series

We attempted to ascertain the correspondence between oxygen isotope stages obtained in marine records and the peaks observed in our $\delta^{18}O$ curve. We

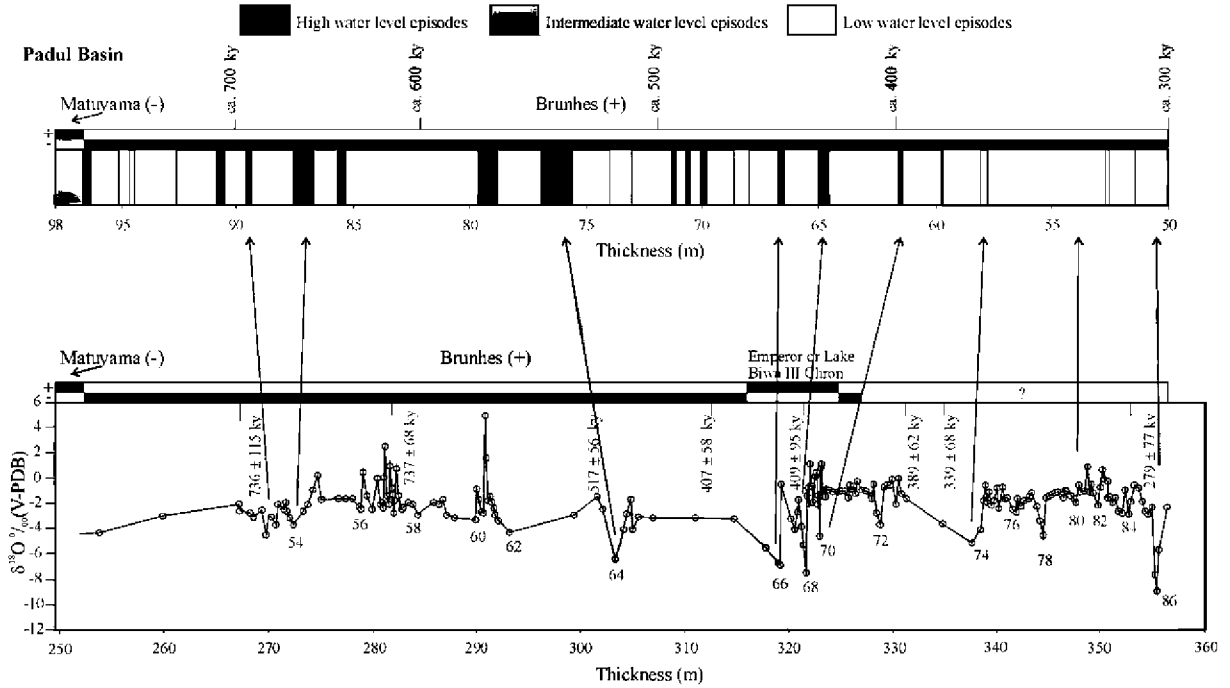

Fig. 12. Correlation between the $\delta^{18}O$ profile of the Guadix-Baza Basin composite section and the paleoenvironmental interpretation of the Padul Basin in terms of water level episodes (cf. Ortiz et al., 2004a,b) from metre 50 (ca. 300 ky B.P.) to metre 98 (ca. 780 ky B.P., Matuyama–Bruhnes boundary). In the Padul Basin profile, estimated ages based on the age–depth relationship established by Ortiz et al. (2004b) has been included.

studied the SPECMAP stack for the interval 0–0.62 my and the OPD site 677 for the interval 0.62–2.0 my (Shackleton, 1995). The magnetic reversal of the base of the Guadix-Baza section (meter 18), which corresponds to the end of the Olduvai Chron (Pliocene–Pleistocene boundary), leads to the correlation of the GB-0 paleoclimatic event defined in the Guadix-Baza sequence with the 64th marine OIS (Fig. 11), which marks the coolest period in the marine record. Some other magnetic reversions along the section, such as the Bruhnes/Matuyama (780 ky) and the Emperor or Lake Biwa III Chrons (ca. 410 ky), lead to correlation of GB-50 and GB-86 paleoclimatic events with the 20th and 8th marine OIS, respectively. The close correspondence between the GB-66 and GB-68 paleoclimatic events and the two maxima that define the 14th marine OIS should also be mentioned.

Near the Guadix-Baza Basin (ca. 60 km eastwards) occurs the Padul Basin that is a subsident fault-bound tectonic endorheic depression of 4 km^2, placed at 720 m and located at the foot of the Sierra Nevada (3000 m). It has one of the best available long records of Pleistocene sediments, with more than 100 m thick, ranging from 1 my to 4.5 ky B.P. Two markedly different hydrogeological scenarios were observed in this basin (Ortiz et al., 2004b) from the concentration of the organic carbon,

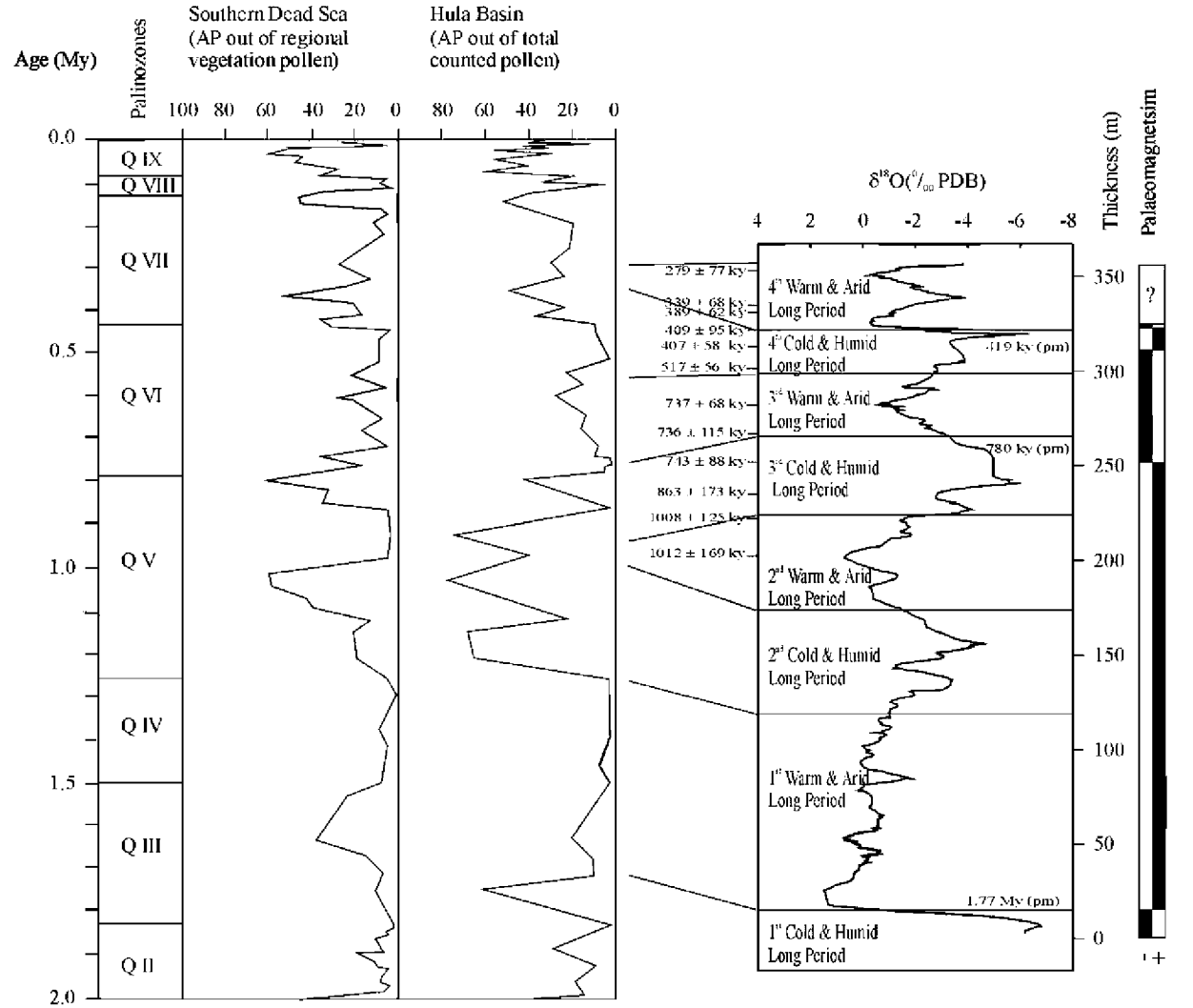

Fig. 13. Correlation between the paleoenvironmental sequence (smoothed $\delta^{18}O$ from *Cyprideis torosa* ostracodes) from the Guadix-Baza Basin composite section and the pollen sequences (percentage of arboreal pollen) obtained in the Southern Dead Sea region and the Hula Basin (Horowitz, 1987, 1989, 2001), both in Israel. The curve for the Hula Basin is mainly based on a pollen diagram from the Notera 3 borehole. The curve for the southern Dead Sea is mainly based on the pollen diagram for the Amazyahu 1 borehole, with additions from Melekh Sdom 1, Ami'az 1, Sdom 2 and Har Sedom 1. The arboreal pollen figure is interpreted as due to increased humidity.

the atomic H/C and C/N ratios, the $\delta^{13}C_{org}$ and CPI values obtained in the sediments: (1) from ca. 1 my B.P. (metre 107) to ca. 400 ka B.P. (metre 60), lacustrine conditions prevailed; and (2) from ca. 400 to 4.5 ky B.P., the Padul Basin became a peat bog. Here, we present (Fig. 12) a correlation between the Guadix-Baza Basin $\delta^{18}O$ record and the corresponding paleoenvironmental interpretation of the Padul Basin in terms of water level episodes (cf. Ortiz et al., 2004b) from metre 50 (ca. 300 ky B.P.) to metre 98 (ca. 780 ky B.P., Matuyama/Bruhnes boundary). As can be observed, there is a general good correspondence between the even paleoclimatic events (cold/humid events) defined in the Guadix-Baza Basin and the high water level episodes distinguished in the Padul Basin. However, there are some spans with a lack of correlation, which will require further study. In fact, it has to be considered the paleohydrogeological behaviour of the Padul Basin as well as its subsidence rate, which should produce high or low water level episodes not exclusively linked to climatic variations.

In the Mediterranean Area, a similar paleoenvironmental evolution is found in the Hula Basin (northern Israel), where Horowitz (1989, 2001) studied a long pollen sequence covering the Pleistocene and most of the Upper Pliocene. He correlated the Pleistocene glaciations with pluvial periods of increased rainfall, while during interglacial episodes, paleoclimatic conditions were more arid. The same good correspondence was also found with a pollen sequence obtained in southern Israel (Southern Dead Sea region) (cf. Horowitz, 1987, 1989, 2001).

The cold–wet and warm–dry episodes defined in Israel can be compared to those in the Guadix-Baza Basin (Fig. 13). The 1st Cold and Humid Period of the Guadix-Baza Basin corresponds to an increase in the percentage of arboreal pollen (higher humidity) in the Hula Basin, whereas the 1st Warm and Dry Period of the Guadix-Baza Basin coincides with low percentages of arboreal pollen in the Hula Basin. In the Southern Dead Sea (Israel), the increase in arboreal pollen occurs between 1.65 and 1.5 my later than in the Hula Basin and the Guadix-Baza Basin. Unfortunately, the pollen record of the Guadix-Baza Basin is extremely poor (Torres et al., 2003b), although silicified Cupressaceae logs have been dated at ca. 600 ky B.P.

Similarly, there is good correspondence between the 2nd, 3rd and 4th Cold and Humid Periods of Guadix-Baza Basin and high percentages of arboreal pollen in both the Southern Dead Sea region and the Hula Basin. Likewise, the 2nd, 3rd and 4th Warm and Dry Periods of the Guadix-Baza Basin correlate closely with low percentages of arboreal pollen in the two sequences from Israel.

Similar paleoenvironmental models have been found in the pluvial lakes developed in the "Basin and Range" area of the United States, such as Owens lake, SE California (Smith and Bischoff, 1997), San Luis Valley, central Colorado (Rogers et al., 1992) and San Felipe Basin, Baja California (Lozano-García et al., 2002), among others. In this area, conditions of less evaporation and higher water availability occurred during cold periods (glacial), while dryness coexisted with warm episodes, causing the development of playa lakes.

6. Conclusions

Long $\delta^{18}O$ and $\delta^{13}C$ profiles obtained in ostracode *C. torosa* valves from the Guadix-Baza Basin (Spain, Mediterranean realm) provide information about global climatic variations at continental middle latitude from ca. 2 my to the upper part of Middle Pleistocene (279 ±77 ky). They result from changes of temperature, evaporation/infill ratios in water bodies and rain amount, producing higher $\delta^{18}O$ and $\delta^{13}C$ values in warm and dry episodes, whereas lower $\delta^{18}O$ and $\delta^{13}C$ values are linked to cold and humid phases. In fact, $\delta^{18}O$ values in the samples accounting for warm–dry phases are higher than those found in present rainwater and in nearby water reservoirs, indicating important evaporation. Similarly, the $\delta^{18}O$ analyzed in waters of shallow lakes developed under semi-arid regimes (Zóñar, Mediana Salada) have positive values, in the range of the highest $\delta^{18}O$ values from the Guadix-Baza Basin. This interpretation was reinforced by the presence of displacive gypsum crystals, which are developed under high salinity and arid stages (evaporative pumping conditions with a saline brine under the lake). In a similar way, the $\delta^{18}O$ and $\delta^{13}C$ oscillations observed in the Ioannina Basin (Greece) and Valle di Castiglione (Italy) records are interpreted in terms of arid/humid climatic phases (Zanchetta et al., 1999; Frogley et al., 1999, 2001). However, the most common isotopic ($\delta^{18}O$) range for the lake is relatively narrow considering the longer period studied (1.6 my). The $\delta^{13}C$ is also affected by plant biomass contribution (amount and type of vegetation—C3 vs. C4 plants), with less biomass and higher percentages of C4 plants during warm and arid episodes. Unfortunately, there is only one study about the palaeodiet of the fauna of the Guadix-Baza Basin, from Venta Micena site (dated at ca. 1 my B.P., cf. Torres et al., 1997; Ortiz et al., 2000), showing that the herbivores (60 samples analysed) fed mainly of C3 plants, based on $\delta^{13}C_{collagen}$ values (Palmqvist et al.,

2003). Nevertheless, the presence of C4 plants during Pleistocene in this area is documented by the palynological studies of Menéndez Amor and Florschütz (1964), Florschütz et al. (1971) and Pons and Reille (1988) carried out in the Padul Basin, which is very close to the Guadix-Baza Basin (ca. 60 km). In any case, the shallow-water bodies installed in the Guadix-Baza Basin, characterized by their extended surface, are sufficient evidences to explain the high $\delta^{13}C$ values due to isotopic exchange and capture of atmospheric CO_2.

Four paleoclimatological scenarios were distinguished: warm and dry (high $\delta^{13}C$ and $\delta^{18}O$ values), cold and humid (low $\delta^{13}C$ and $\delta^{18}O$ values), temperate–dry (intermediate $\delta^{18}O$ and high $\delta^{13}C$ values) and temperate–humid (intermediate $\delta^{18}O$ and low $\delta^{13}C$ values).

In general, there is covariation between $\delta^{18}O$ and $\delta^{13}C$ signals, which is typical of arid and semi-arid areas and closed basins. However, $\delta^{13}C$ signals show good correlation with other paleoclimatological series located in different areas of middles latitudes, indicating an important global component, such as atmospheric CO_2 concentration (different greenhouse scenarios). Interglacial Quaternary warm climates are related with increasing atmospheric CO_2 concentration (Petit et al., 1999) and global wetter conditions. However, in middle latitudes from Mediterranean areas and North America, the increasing of temperature is associated with drier conditions (Horowitz, 1989, 2001; Menking et al., 2004).

Likewise, four Cold and Humid Long Periods alternating with four Warm and Dry Long Periods were established from the smoothed $\delta^{18}O$ ostracode curve. Climate worsening (warm–dry conditions) seems to be a faster process than the following climate improvements (cold–humid episodes). These alternating "warm and dry" and "cold and humid" episodes diverge from the paleoclimatological record of the Northern Hemisphere. In fact, the Guadix-Baza Basin is located in the Mediterranean area where glacial periods did not cause permafrost conditions and scarce water, such as occurred in northern Europe. In the Mediterranean region during glacial episodes, higher precipitation would occur.

A total of 88 climatic events, representing either warm–dry conditions (odd events) or cold–humid episodes (even events) were distinguished for the $\delta^{18}O$ and $\delta^{13}C$ profiles in the Guadix-Baza section. Close correlation between the Guadix-Baza Basin and both the deep-sea oxygen-isotope record (SPECMAC-OPD677) was obtained. There is also good correspondence with basins in the Mediterranean area (Horowitz, 1987, 1989, 2001). Similar paleoenvironmental models have been found in North America pluvial lakes. This indicates that climate at the Guadix-Baza Basin responded to global climate changes.

Acknowledgements

Funding was obtained from the projects "Evolución Paleoclimática de la Mitad Sur de la Península Ibérica" of ENRESA (National Company for Radioactive Waste Management), "Evidence from Quaternary Infills Paleohydrology" (EQUIP) of the European Union (F14W/CT96/0031), and REN2001-1874 and REN2003-05199 grants from the Spanish Ministry of Science and Technology. We thank Profs. Aharon Horowitz, Baruch Spiro and Paul De Deckker for their helpful comments on the manuscript.

Appendix A

$\delta^{13}C$ (‰ V-PDB)	$\delta^{18}O$ (‰ V-PDB)	Depth (m)	Estimated age (ky)
−6.41	−6.16	2.50	1941
−9.05	−8.33	4.00	1934
−9.68	−7.98	6.00	1925
−9.57	−6.05	6.50	1922
−5.17	−0.95	13.20	1891
−4.94	0.11	13.50	1889
−4.57	−1.17	15.10	1882
−3.25	0.94	16.50	1875
−3.53	0.19	17.30	1871
−3.96	−0.93	25.20	1834
−4.10	−1.30	25.50	1833
−3.98	−1.20	25.90	1831
−2.71	−0.18	31.30	1805
−2.48	0.00	35.00	1788
−3.13	−0.06	35.50	1785
−4.42	−0.18	38.70	1770
−4.31	−0.49	40.10	1764
−4.04	0.97	40.30	1763
−4.50	−0.60	40.90	1760
−3.67	−0.06	41.30	1758
−3.48	0.20	42.20	1754
−2.97	−0.29	42.60	1752
−3.42	1.54	42.90	1751
−2.72	0.27	43.20	1749
−4.67	−0.71	43.50	1748
−2.38	−0.87	43.80	1746
−4.11	−0.77	44.00	1745
−3.19	−2.01	44.15	1745
−3.14	−0.88	44.30	1744
−2.87	0.31	44.50	1743
−2.75	−0.98	44.60	1743
−2.65	−0.37	44.80	1742
−3.04	−0.09	45.20	1740
−2.70	−0.24	45.40	1739
−3.31	−0.69	45.60	1738
−3.29	−0.32	45.90	1736

(continued on next page)

Appendix A (*continued*)

$\delta^{13}C$ (‰ V-PDB)	$\delta^{18}O$ (‰ V-PDB)	Depth (m)	Estimated age (ky)
−3.54	0.98	46.30	1734
−3.30	0.19	46.60	1733
−3.58	0.10	46.90	1732
−3.53	1.51	47.20	1730
−3.08	1.59	47.50	1729
−3.59	−0.50	48.30	1725
−3.69	0.18	49.30	1720
−3.73	1.37	49.60	1719
−2.50	−0.68	50.80	1713
−2.29	0.74	51.10	1712
−2.66	1.31	51.40	1710
−3.09	0.70	51.60	1709
−2.81	−0.22	51.80	1709
−2.50	1.55	52.10	1707
−2.22	−0.69	52.90	1703
−4.30	−0.65	54.60	1695
−2.75	−1.30	55.50	1691
−3.21	−1.28	55.80	1690
−2.89	−2.86	56.30	1687
−3.54	−1.15	56.80	1685
−3.30	0.13	57.30	1683
−4.58	0.97	57.80	1680
−3.78	−1.58	58.20	1678
−3.57	0.58	58.50	1677
−2.98	−0.48	58.90	1675
−3.73	−0.03	59.30	1673
−3.33	−0.37	59.70	1671
−2.86	−0.76	63.00	1656
−2.88	−0.91	63.50	1653
−2.70	0.33	64.00	1651
−4.10	−1.50	64.50	1649
−3.10	−0.10	65.10	1646
−2.70	−0.30	65.20	1645
−2.71	0.08	66.30	1640
−3.41	−0.13	67.00	1637
−5.76	0.41	67.50	1634
−5.25	−0.70	69.60	1625
−4.71	−0.30	71.90	1614
−4.53	−0.17	74.80	1600
−3.91	0.30	77.60	1587
−3.96	1.19	77.90	1585
−4.02	−1.09	78.10	1584
−3.48	0.47	78.40	1583
−3.99	−0.48	78.70	1582
−2.00	−0.31	79.40	1578
−3.26	−0.70	79.80	1576
−2.63	−0.12	80.30	1574
−4.20	0.13	80.80	1572
−4.27	−2.22	81.20	1570
−4.78	−1.35	81.60	1568
−4.84	−1.32	81.80	1567
−4.43	−2.66	84.60	1554
−3.98	0.55	84.50	1554
−4.33	0.08	89.10	1533
−4.74	−0.48	94.10	1509
−5.24	−0.27	94.50	1507
−3.78	−1.21	95.80	1501

Appendix A (*continued*)

$\delta^{13}C$ (‰ V-PDB)	$\delta^{18}O$ (‰ V-PDB)	Depth (m)	Estimated age (ky)
−5.18	−0.41	96.10	1500
−3.76	−0.69	96.60	1497
−2.98	0.37	97.00	1495
−4.44	1.10	97.70	1492
−3.43	0.19	98.10	1490
−4.18	−0.35	98.20	1490
−4.33	−0.44	98.70	1487
−3.69	−0.77	99.00	1486
−4.07	0.87	99.40	1484
−5.54	0.38	101.10	1476
−6.34	−3.12	101.70	1473
−4.13	−1.16	102.60	1469
−3.73	−1.03	104.50	1460
−5.57	0.36	105.30	1456
−4.77	−1.34	106.20	1452
−4.62	−1.11	107.20	1447
−4.74	−0.28	107.60	1445
−3.81	1.56	108.40	1442
−6.17	−2.12	108.70	1440
−4.90	−0.40	109.20	1438
−7.89	−2.41	109.80	1435
−5.60	−1.30	110.30	1433
−5.29	−1.03	110.80	1430
−5.41	−0.69	111.40	1427
−5.08	−0.45	111.80	1426
−4.39	−0.19	112.10	1424
−4.63	0.94	112.30	1423
−2.92	−0.65	113.10	1419
−5.67	−1.22	113.50	1418
−4.00	−0.05	114.00	1415
−5.35	−0.27	114.50	1413
−8.19	−1.08	115.40	1409
−3.75	−1.45	116.30	1404
−6.99	−2.83	116.50	1403
−7.13	−1.57	116.90	1401
−5.21	−0.52	117.00	1401
−5.04	−1.20	120.50	1384
−3.74	−1.65	121.40	1380
−4.95	−2.24	121.80	1378
−4.88	−1.07	122.50	1375
−4.10	−0.83	123.20	1372
−3.30	0.32	123.80	1369
−6.08	−0.11	124.30	1367
−7.19	−3.14	125.90	1359
−7.76	−1.72	126.80	1355
−9.10	−4.82	127.30	1352
−5.73	−2.36	128.00	1349
−4.50	−0.55	129.00	1344
−4.74	−0.39	130.00	1340
−7.69	−5.28	131.10	1334
−7.47	−4.73	131.20	1334
−6.59	−2.53	133.90	1321
−7.96	−2.51	136.40	1309
−5.27	−1.20	136.70	1308
−5.10	−0.80	137.50	1304
−5.06	−0.08	138.50	1300
−5.55	0.04	139.20	1296

Appendix A (*continued*)

$\delta^{13}C$ (‰ V-PDB)	$\delta^{18}O$ (‰ V-PDB)	Depth (m)	Estimated age (ky)
−6.04	0.16	140.00	1293
−4.30	−0.14	141.00	1288
−5.23	−0.19	141.60	1285
−5.84	−0.72	141.90	1284
−5.54	−0.98	142.20	1282
−3.86	−0.05	142.60	1280
−6.06	−2.84	142.80	1279
−5.50	−0.80	143.10	1278
−8.13	−2.36	143.50	1276
−8.42	−1.84	143.80	1275
−5.91	−1.95	144.40	1272
−8.18	−5.53	144.90	1269
−7.27	−4.23	147.00	1259
−6.36	−2.92	148.40	1253
−5.14	−1.19	150.20	1244
−5.96	−3.10	151.20	1240
−7.20	−5.97	152.00	1236
−6.62	−3.67	153.90	1227
−6.71	−2.18	154.30	1225
−7.27	−4.87	155.10	1221
−7.55	−6.22	155.50	1219
−5.15	−1.21	156.00	1217
−6.31	−1.19	157.10	1212
−8.63	−1.14	161.70	1190
−6.37	−1.67	162.70	1185
−4.21	−1.84	164.20	1178
−5.83	−2.63	164.90	1175
−3.32	1.08	168.50	1158
−6.50	−1.16	171.00	1146
−4.39	−0.37	173.00	1137
−5.94	−2.73	174.20	1131
−5.03	−0.18	174.90	1128
−5.52	−1.58	175.60	1125
−5.51	−0.48	176.10	1122
−4.25	−1.24	178.00	1113
−5.53	−0.39	179.00	1109
−4.21	−1.56	179.50	1106
−4.27	−1.19	182.00	1094
−4.36	−0.65	185.50	1078
−4.68	−2.18	186.10	1075
−5.73	−2.91	187.50	1068
−5.98	−1.17	188.00	1066
−4.34	−1.72	188.30	1065
−6.35	−1.95	188.60	1063
−4.99	−2.05	189.20	1060
−5.06	−1.18	192.00	1047
−5.16	0.13	193.70	1039
−4.41	0.38	197.90	1019
−4.00	0.52	200.60	1007
−4.68	−0.31	202.20	999
−5.54	−1.36	205.30	984
−6.81	−1.38	206.60	978
−7.71	−5.49	212.00	953
−4.49	−0.34	212.40	951
−4.07	−1.66	212.70	950
−4.11	−0.42	213.10	948

Appendix A (*continued*)

$\delta^{13}C$ (‰ V-PDB)	$\delta^{18}O$ (‰ V-PDB)	Depth (m)	Estimated age (ky)
−4.33	−1.03	213.50	946
−4.04	−0.50	213.90	944
−4.24	0.87	214.40	942
−2.92	0.52	214.60	941
−4.73	−2.49	215.60	936
−4.98	−1.43	217.00	929
−5.55	−1.70	217.50	927
−4.84	−0.30	217.90	925
−4.93	−1.15	218.30	923
−5.04	−1.32	218.80	921
−3.30	−0.59	219.60	917
−4.20	−0.59	220.10	915
−3.84	−0.57	220.40	913
−4.37	−1.47	220.80	911
−5.87	−2.60	221.40	909
−5.41	−1.61	221.50	908
−9.58	−11.08	223.80	897
−8.00	−2.03	224.70	893
−8.53	−6.00	225.70	888
−4.17	−0.25	226.70	884
−4.26	0.08	229.40	871
−6.74	−3.33	230.00	868
−5.18	−1.02	230.50	866
−4.63	−1.08	231.00	863
−4.43	−0.92	231.50	861
−7.54	−5.21	236.30	838
−9.40	−7.78	238.50	828
−9.00	−8.16	239.30	824
−9.14	−8.28	239.70	822
−3.80	−1.80	240.60	818
−3.10	−4.50	242.30	810
−2.90	−2.20	242.40	809
−3.70	−3.90	244.00	802
−4.00	−4.80	244.70	799
−4.11	−3.79	257.10	740
−4.17	−3.28	259.20	730
−4.30	−2.10	267.00	693
−3.10	−2.60	267.30	692
−4.50	−3.00	268.60	686
−4.40	−2.60	269.30	683
−4.12	−4.47	269.70	681
−3.50	−3.10	270.00	679
−4.10	−3.10	270.30	678
−4.80	−3.70	270.70	676
−4.30	−2.10	270.90	675
−3.60	−2.50	271.40	673
−3.00	−1.90	271.60	672
−2.80	−2.60	271.70	671
−3.80	−3.70	272.40	668
−4.40	−2.10	273.70	662
−2.80	0.20	274.70	657
−4.30	−1.70	275.10	655
−3.90	−1.60	278.00	642
−3.00	−2.50	278.90	637
−6.60	0.40	279.10	636
−3.50	−1.40	279.50	634

(continued on next page)

Appendix A (*continued*)

$\delta^{13}C$ (‰ V-PDB)	$\delta^{18}O$ (‰ V-PDB)	Depth (m)	Estimated age (ky)
−5.30	−2.50	279.90	633
−2.70	0.00	280.40	630
−4.30	−2.10	280.70	629
−3.60	−1.90	280.90	628
−4.80	−2.40	281.00	627
−4.10	2.50	281.20	626
−3.60	−1.40	281.40	626
−7.40	−2.10	281.60	625
−2.80	1.00	281.70	624
−2.80	−0.80	281.80	624
−4.40	−1.30	281.90	623
−5.00	−2.80	282.00	623
−3.40	−1.80	282.10	622
−3.40	0.70	282.30	621
−4.70	−1.40	282.50	620
−3.50	−2.50	282.80	619
−4.70	−2.30	282.90	618
−3.40	−1.90	283.40	616
−3.10	−2.10	283.90	614
−3.70	−2.90	284.30	612
−6.60	−1.90	285.90	604
−6.40	−2.10	286.30	602
−5.40	−1.70	286.70	601
−3.70	−2.90	287.10	599
−4.70	−3.17	287.90	595
−5.20	−3.30	289.90	585
−4.50	−0.90	290.00	585
−5.60	−1.70	290.20	584
−5.50	−2.70	290.40	583
−3.70	−2.80	290.60	582
−3.90	4.90	290.80	581
−3.40	−1.80	291.10	580
−4.60	−1.50	291.30	579
−4.70	−2.40	291.70	577
−3.80	−2.90	291.80	576
−4.33	−3.83	292.60	573
−4.60	−4.30	293.10	570
−4.20	−3.37	296.40	555
−3.40	−1.50	301.50	531
−4.90	−2.50	302.10	528
−7.70	−6.40	303.30	522
−5.85	−4.05	304.10	518
4.92	−2.87	304.40	517
−4.00	−1.70	304.80	515
−4.20	−4.10	305.00	514
−3.60	−3.10	305.50	512
−3.66	−3.13	308.50	498
−3.71	−31.50	310.60	488
−3.80	−3.20	314.70	468
−4.85	−4.76	316.70	459
−6.30	−6.90	319.20	447
−4.30	−0.50	319.30	447
−4.55	−3.50	320.30	442
−4.60	−4.10	320.50	441
−3.70	−2.66	320.80	440
−3.10	−1.70	320.90	439
−3.85	−3.87	321.20	438

Appendix A (*continued*)

$\delta^{13}C$ (‰ V-PDB)	$\delta^{18}O$ (‰ V-PDB)	Depth (m)	Estimated age (ky)
−3.85	−3.87	321.30	437
−5.10	−7.50	321.70	435
−3.50	−1.40	321.80	435
−2.50	−0.80	321.90	434
−3.70	−2.00	322.00	434
−3.60	1.10	322.10	434
−2.40	−0.60	322.20	433
−2.40	−0.60	322.30	433
−2.00	−1.90	322.40	432
−2.40	0.10	322.50	432
−3.80	0.40	322.60	431
−2.60	−2.10	322.70	431
−2.50	−1.40	322.80	430
−4.00	−4.60	322.90	430
−2.80	0.80	323.00	429
−1.50	1.10	323.10	429
−2.60	−1.40	323.20	428
−3.60	−1.10	323.30	428
−4.30	−1.20	323.40	427
−2.40	−1.50	323.50	427
−5.60	−0.90	323.60	426
−4.78	−0.93	323.90	425
−5.26	−1.11	324.30	423
−4.78	−0.99	325.40	418
−4.46	−1.56	325.70	417
−4.14	−0.58	325.90	416
−7.19	−0.90	326.00	415
−5.49	−0.65	326.20	414
−5.10	−1.21	326.40	413
−4.55	−0.23	326.60	412
−4.55	−0.97	327.00	410
−4.67	−1.02	327.40	409
−6.26	−1.36	327.90	406
−6.23	−1.60	328.00	406
−4.20	−0.52	328.20	405
−6.21	−2.76	328.50	403
−6.73	−3.70	328.80	402
−4.57	−0.73	329.10	401
−3.74	−0.59	329.40	399
−4.34	−0.58	329.70	398
−4.07	−0.07	329.90	397
−3.74	−2.09	330.30	395
−4.41	0.01	330.60	393
−4.84	−1.26	330.90	392
−7.07	−3.99	335.80	369
−7.70	−4.78	336.80	364
−8.02	−5.17	337.60	360
−4.46	−1.75	338.70	355
−3.11	−0.53	338.90	354
−4.04	−1.97	339.10	353
−5.08	−1.06	339.30	352
−5.84	−2.17	339.50	351
−5.70	−1.81	339.70	351
−6.45	−0.79	340.00	349
−6.42	−2.37	340.20	348
−5.99	−0.73	340.60	346
−6.66	−1.65	340.80	345

Appendix A (*continued*)

$\delta^{13}C$ (‰ V-PDB)	$\delta^{18}O$ (‰ V-PDB)	Depth (m)	Estimated age (ky)
−4.89	−1.57	341.00	344
−4.88	−2.50	341.50	342
−6.23	−2.70	341.80	341
−3.73	−1.66	341.95	340
−4.04	−2.13	342.10	339
−4.07	−2.21	342.30	338
−4.30	−1.80	342.60	337
−5.78	−1.18	343.40	333
−6.12	−3.35	344.10	330
−7.23	−4.55	344.40	328
−4.42	−1.55	344.70	327
−4.99	−1.40	345.00	326
−6.72	−1.10	345.90	321
−4.65	−1.57	346.40	319
−4.29	−0.96	346.60	318
−4.69	−1.03	346.75	317
−6.27	−1.42	347.10	316
−5.53	−1.64	347.40	314
−6.23	−1.89	347.60	313
−5.11	−0.59	347.85	312
−5.63	−1.09	348.10	311
−3.72	−1.00	348.40	309
−8.33	0.90	348.70	308
−9.26	−1.11	348.90	307
−8.86	−0.45	349.10	306
−9.76	−1.19	349.30	305
−8.82	−2.17	349.80	303
−5.89	0.69	350.15	301
−6.53	−0.07	350.35	300
−4.08	−0.27	350.60	299
−4.79	−1.54	350.60	299
−5.21	−1.45	350.80	298
−5.89	−1.92	351.10	297
−4.87	−1.52	351.40	295
−5.90	−2.65	351.70	294
−6.00	−2.77	352.05	292
−3.58	−0.94	352.40	291
−4.73	−2.87	352.70	289
−4.60	−1.84	352.90	288
−1.89	−0.56	353.20	287
−3.49	−0.79	353.60	285
−3.57	−1.83	354.00	283
−4.55	−2.65	354.30	282
−3.99	−2.87	354.60	280
−4.57	−2.28	354.90	279
−4.41	−7.64	355.20	277
−5.32	−8.98	355.40	276
−6.71	−2.28	356.40	271

References

Agustí, J., 1986. Synthèse biostratigraphique du Plio-Pléistocène de Guadix-Baza (Province de Granada, Sud-est de l'Espagne. Geobios 19 (4), 505–510.

Anadón, P., De Deckker, P., Julià, R., 1986. The Pleistocene lake deposits of the NE Baza Basin (Spain): salinity variations and ostracod succession. Hydrobiologia 143, 199–208.

Anadón, P., Utrilla, R., Julià, R., 1994. Palaeoenvironmental reconstruction of a Pleistocene lacustrine sequence from faunal assemblages and ostracode shell geochemistry, Baza Basin, SE Spain. Palaeogeogr. Palaeoclimatol. Palaeoecol. 111, 191–205.

Bade, D.L., Carpenter, S.R., Cole, J.J., Hanson, P.C., Hesslein, R.H., 2004. Controls of delta C-13-DIC in lakes: geochemistry, lake metabolism, and morphometry. Limnol. Oceanogr. 49, 1160–1172.

Belatini de, P.C.M., 1959. Oxygen isotope variations in Antarctic snow samples. Nature 184, 1557–1559.

Bonadonna, F.P., Leone, G., 1989. La Región de Guadix-Baza: datos de la composición isotópica del oxígeno y del carbono y reconstrucción paleoambiental. In: Alberdi, M.T., Bonadonna, F. P. (Eds.), Geología y Paleontología de la cuenca de Guadix-Baza. Trabajos sobre Neógeno-Cuaternario, vol. 11, pp. 79–98.

Boomer, I., 1993. Palaeoenvironmental indicators from Late Holocene and contemporary ostracoda of the Aral Sea. Palaeogeogr. Palaeoclimatol. Palaeoecol. 103, 141–153.

Bordegat, A.M., 1979. Teneurs relative en phosphore, potassium et aluminium dans le caparace d'ostracodes actuels. Intérêt écologique (Analyse à la microsonde électronique). In: Krstic, N. (Ed.), Taxonomy, Biostratigraphy and Distribution of Ostracodes. Proceedings of the 7th International Symposium on Ostracodes. Serbian Geological Society, Belgrade, pp. 261–264.

Bordegat, A.M., 1985. Composition chimique des carapaces d'Ostracodes. Paramètres du milieu de vie. Atlas des Ostracodes de France. Bull. Centres Rech. Explor. Prod. Elf-Aquitaine, Pau, vol. 9, pp. 379–386.

Broecker, W.S., 1992. The Glacial World According to Wally. Lamont-Doherty Geological Observatory of Columbia University, Palisades. 258 pp.

Cadot, H.M., Kaesler, R.L., 1977. Magnesium content of calcite in caparaces of benthic marine Ostracoda. Univ. Kans. Paleontol. Contrib. 87, 1–23.

Calvache, M.L., Viseras, C., 1997. Long-term control mechanisms of stream piracy processes in southeast Spain. Earth Surf. Proc. Landf. 22, 93–105.

Cande, S.C, Kent, D.V., 1995. Revised calibration of the geomagnetic polarity time scale for the late Cretaceous and Cenozoic. J. Geophys. Res. 100, 6093–6095.

Carbonnel, G., 1983. Morphométre et hypersalinité chez *Cyprideis torosa* (Jones) (*Ostracoda*, Actuel) dans les salines de Santa-Pola (Alicante, Espagne). Sci. Géol. Bull. 36 (4), 211–219.

Cerling, T.E., 1984. The stable isotopic composition of modern sil carbonate and its relationship to climate. Earth Planet. Sci. Lett. 71, 229–240.

Cerling, T.E., 1991. Carbon dioxide in the atmosphere: evidence from Cenozoic and Mesozoic paleosols. Am. J. Sci. 291, 377–400.

Chivas, A., De Deckker, P., Shelley, J.M., 1983. Magnesium, strontium and barium partioning in nonmarine ostracode shells and their use in paleoenvironmental reconstructions—A preliminary study. In: Maddocks, R.F. (Ed.), Applications of Ostracoda. 8th International Symposium Ostracoda. University of Houston Geosciences, Houston, pp. 238–249.

Chivas, A.R., De Deckker, P., Wang, S.X., Cali, J.A., 2002. Oxygen-isotope Systematics of the Nektic Ostracod *Australocypris robusta*. In: Holmes, J.A., Chivas, A.R. (Eds.), Applications of the Ostracoda to Quaternary Research. Am. Geophysical Union Geophysical Monograph, vol. 131, pp. 301–313.

Coplen, T.B., Winograd, I.J., Landwehr, J.M., Riggs, A.C., 1994. 500,000-year stable carbon isotopic record from Devils Hole, Nevada. Science 263, 361–365.

Craig, H., 1965. The measurement of oxygen isotope paleotemperatures. In: Tongiorgi, E. (Ed.), Stable Isotopes in Oceanographic Studies and Paleotemperatures. Proceedings of the Spoleto Conference. Consiglio Nazionale delle Ricerche, Pisa, pp. 3–24.

Dansgaard, W., 1964. Stable isotopes in precipitation. Tellus 5 (16), 461–469.

Dansgaard, W., Johnsen, S.J., Clausen, H.B., Dahl-Jensen, D., Gundestrup, N.S., Hammer, C.U., Hvidberg, C.S., Steffensen, J. P., Sveinbjörnsdottir, A.E., Jouzel, J., Bond, G., 1993. Evidence for general instability of past climate from a 250-kyr ice-core record. Nature 364, 218–220.

de Beaulieu, J.L., Reille, M., 1984. A long upper-Pleistocene pollen record from Les Echets near Lyon, France. Boreas 13, 111–132.

de Beaulieu, J.L., Reille, M., 1992a. The last climatic cycle at La Grande Pile (Vosges, France). A new pollen profile. Quat. Sci. Rev. 11, 431–438.

de Beaulieu, J.L., Reille, M., 1992b. Long Pleistocene sequences from the Velay plateau (Massif Central, France): I. Ribains maar. Veg. Hist. Archaeobot. 1, 233–242.

De Deckker, P., 1981. Ostracods of athalassic saline lakes. Hydrobiologia 81, 131–144.

Dean, W.E., Stuiver, M., 1993. Stable carbon and oxigen isotope studies of the sediments of Elk Lake, Minnesota. In: Bradbury, J.P., Dean, W.E. (Eds.), Elk Lake, Minnesota: Evidence for Rapid Climate Change in the North-Central United States. Geol. Soc. Am., Spec. Paper, vol. 276, pp. 163–180.

Deines, P., 1980. The isotopic composition of reduced organic carbon. In: Fritz, P., Fontes, J.Ch. (Eds.), Handbook of Environmental Isotope Geochemistry, vol. 1, pp. 329–406.

Delgado, A., 1994. Estudio isotópico de los procesos diagenéticos e hidrotermales relacionados con la génesis de bentonitas (Cabo de Gata, Almería). PhD thesis, Universidad de Granada. 413 pp.

Delgado, A., Reyes, E., 2001. Oxygen and hydrogen isotopes as paleoclimatic indicators in continental environments: III. Congreso Ibérico de Geoquímica, pp. 235–239.

Delgado, A., Núñez, R., Caballero, E., Jiménez de Cisneros, C., Reyes, E., 1991. Composición isotópica del agua de lluvia en Granada. IV Congreso Geoquímica España 1, 350–358.

Dettman, D.L., Smith, A.J., Rea, D.K., Moore, T.C., Lohmann, K., 1995. Glacial Meltwater in Lake Huron during Early Postglacial Time as Inferred from Single-Valve Analysis of Oxygen Isotopes in Ostracodes. Quat. Res. 43, 297–310.

Durazzi, J.T., 1977. Stable isotopes in the ostracod shell: a preliminary study. Geochim. Cosmochim. Acta 41, 1168–1170.

EPICA group, 2004. Eight glacial cycles from an Antarctic ice core. Nature 429, 623–628.

Eyles, N., Schwarcz, H.P., 1991. Stable isotope record of the last glacial cycle from lacustrine ostracodes. Geology 19, 257–260.

Florschütz, F., Menéndez Amor, J., Wijmstra, T.A., 1971. Palinology of a thick Quaternary succession in southern Spain. Palaeogeogr. Palaeoclimatol. Palaeoecol. 10, 233–264.

Follieri, M., Madri, P., Sadori, L., 1988. 250,00-year pollen record from valle di Castiglione (Roma). Pollen et Spores 30, 329–356.

Fontes, J.Ch., Edmunds, W.M., 1989. The use of environmental isotope techniques in arid zone hydrolgy. A critical review. Technical Documents in Hydrology. UNESCO, pp. 1–75.

Fontes, J.Ch., Gasse, F., Callot, Y., Plaziat, J.-C., Carbonel, P., Dupeuble, P.A., Kaczmarska, I., 1985. Freshwater to marine-like environments from Holocene lakes in northern Sahara. Nature 317, 608–610.

Friedli, H., Lotscher, H., Oeschger, H., Stauffer, B., 1986. Ice core record of the $^{13}C/^{12}C$ ratio of atmospheric CO_2 in the past two centuries. Nature 324, 237–238.

Fritz, S.C., Baker, P.A., Lowenstein, T.K., Seltzer, G.O., Rigsby, C.A., Dwyer, G.S., Tapia, P.M., Arnold, K.K., Ku, T.L., Luo, S., 2003. Hydrologic variation during the last 170,000 years in the southern hemisphere tropics of South America. Quat. Res. 61 (1), 95–104.

Frogley, M.R., Tzedakis, P.C., Heaton, T.H.E., 1999. Climate variability in northwest Greece during the last interglacial. Science 285, 1886–1889.

Frogley, M.R., Griffiths, H.I., Heaton, T.H.E., 2001. Historical biogeography and Late Quaternary environmental change of Lake Pamvotis, Ioannina (north-western Greece): evidence from ostracods. J. Biogeogr. 28, 745–756.

Gasse, F., Fontes, J.C., Plaziat, J.C., Carbonel, P., Kaczmarska, I., De Deckker, P., Soulié-Marsche, I., Callot, Y., Dupeuble, P.A., 1987. Biological remains, geochemistry and stable isotopes for the reconstruction of environmental and hydrological changes in the Holocene lakes from North Sahara. Paleogeogr. Paleoclimatol. Paleoecol. 60, 1–46.

Gonfiantini, R., 1981. Stable isotope hydrology. IAEA Tech. Rep. 210, 35–84.

Grootes, P.M., Steig, E.J., Stuiver, M., Waddington, E.D., Morse, D.L., 2001. The Taylor Dome Antartic ^{18}O record and globally synchronous changes in climate. Quat. Res. 56, 289–298.

Guerra Merchán, A., 1990. Sobre la conexión entre la Depresión de Guadix-Baza y el Corredor del Almanzora. (Cordilleras Béticas, Andalucía Oriental). Geogaceta 8, 97–99.

Hauser, S., Dongarrá, G., Favara, R., Longinelli, A., 1980. Composizione isotopica delle piogge in Sicilia. Riferimenti di base per studi hidrogeologici e relazioni con altre aree mediterranee. Rend. Soc. Ital. Mineral. Petrol. 36 (2), 650–671.

Heaton, T.H.E., Holmes, J.A., Bridgwater, N.D., 1995. Carbon and oxygen isotope variations among lacustrine ostracods: implications for paleoclimatic studies. The Holocene 5 (4), 428–434.

Heip, C., 1976. The life-cycle of *Cyprideis torosa* (Crustacea, Ostracoda). Oecologia 24, 229–245.

Holmes, J.A., Street-Perrott, F.A., Allen, M.J., Fothergill, P.A., Harkness, D.D., Kroon, D., Perrott, R.A., 1997. Holocene palaeolimnology of Kajemuran Oasis, Northern Nigeria: an isotopic study of ostracodes, bulk carbonate and organic carbon. J. Geol. Soc. (Lond.) 154, 311–319.

Hooghiemstra, H., Melice, J.L., Berger, A., Shackleton, N.J., 1993. Frequency spectra and paleoclimatic variability of the high-resolution 30–1450 ka Funza I Pollen Record (Eastern Cordillera, Colombia). Quat. Sci. Rev. 12, 141–156.

Horowitz, A., 1987. Subsurface Palynostratigraphy and Paleoclimates of the Quaternary Jordan Rift Valley Fill, Israel. Isr. J. Earth-Sci. 36, 31–44.

Horowitz, A., 1989. Continous pollen diagrams from the last 3.5 m.y. from Israel: vegetation, climate and correlation with the oxygen isotope record. Palaeogeogr. Palaeoclimatol. Palaeoecol. 72 (1–2), 63–78.

Horowitz, A., 2001. The Jordan Rift Valley. Balkema, Amsterdam. 730 pp.

Jouzel, J., Barkov, N.I., Barnola, J.M., Bender, M., Chappelaz, J., Genthon, C., Kotlyakov, V.M., Lipenkov, V., Lorius, C., Petit, J.R., Raynaud, D., Raisbeck, G., Ritz, C., Sowers, T., Stievenard, M., Yiou, F., Yiou, P., 1993. Extending the Vostok ice-core record of paleoclimate to the penultimate glacial period. Nature 364, 407–412.

Kashiwaya, K., Matsumoto, G.I., Takamatsu, T., Minoura, K., Takahara, H., Kawai, T., 2003. Long Continental Records from Lake Baikal. Springer-Verlag, Tokyo. 370 pp.

Keatings, K.W., Heaton, T.H.E., Holmes, J.A., 2002. Carbon and oxygen isotope fractionation in non-marine ostracods: Results

from a 'natural culture' environment. Geochim. Cosmochim. Acta 66 (10), 101–1711.

Kershaw, A.P., 1986. Climatic change and Aboriginal burning in north-east Australia during the last two glacial/interglacial cycles. Nature 322, 47–49.

Kim, S.T., O'Neil, J.R., 1987. Equilibrium and nonequilibrium oxygen isotope effects in synthetic carbonates. Geochim. Cosmochim. Acta 61, 3461–3475.

Li, H.-C., Ku, T.-L., 1997. $\delta^{13}C$–$\delta^{18}O$ covariance as a paleohydrological indicator for closed-basin lakes. Palaeogeogr. Palaeoclimatol. Palaeoecol. 133, 69–80.

Lister, G.S., 1988. Stable isotopes from lacustrine ostracoda as tracers for continental palaeoenvironments. In: De Deckker, P., Colin, J.P., Peypouquet, J.P. (Eds.), Ostracoda in the Earth Sciences. Eselvier, pp. 201–218.

Lister, G.S., Kelts, K., Zao, C.K., Yu, J.-Q., Niessen, F., 1991. Lake Quinghai, China: closed-basin lake levels and the oxygen isotope record for ostracoda since the latest Pleistocene. Palaeogeogr. Palaeoclimatol. Palaeoecol. 84, 141–162.

Longinelli, A., Selmo, E., 2003. Isotopic composition of precipitation in Italy: a first overall map. J. Hydrol. 270, 75–88.

Lozano-García, M.S., Ortega-Guerrero, B., Sosa-Nájera, S., 2002. Mid- to late-Wisconsin pollen record of San Felipe Basin, Baja California. Quat. Res. 58, 84–92.

McCrea, J.M., 1950. On the isotopic chemistry of carbonates and a paleotemperature scale. J. Chem. Phys. 18, 849–857.

Mees, F., Reyes, E., Keppens, E., 1998. Stable isotope chemistry of gaylussite and nahcolite from the deposits of the crater lake at Malha, northern Sudan. Chem. Geol. 146, 87–98.

Menéndez Amor, J., Florschütz, F., 1964. Results of the preliminary palynological investigation of samples from a 50m boring in southern Spain. Bol. R. Soc. Esp. Hist. Nat. (Geol.) 62, 251–255.

Menking, K.M., Anderson, R.Y., Shafike, N.G., Syed, K.H., Allen, B.D., 2004. Wetter or colder during the last glacial maximum? Revisiting the pluvial lake question in southwestern north America. Quat. Res. 62, 280–288.

Mezquita, F., Olmos, V., Oltra, R., 2000. Population ecology of *Cyprideis torosa* (Jones, 1850) in a hypersaline environment of the western mediterranean (Santa Pola, Alacant). Ophelia 53 (2), 119–130.

Millán, M.M., Estrela, M.J., Sanz, M.J., Mantilla, E., Martín, M., Pastor, F., Salvador, R., Vallejo, R., Alonso, L., Gangoiti, G., Ilardia, J.L., Navazo, M., Albizuri, A., Artíñano, B., Ciccioli, P., Kallos, G., Carvalho, R.A., Andrés, D., Hoff, A., Werhahn, J., Seufert, G., Versino, B., 2005. Climatic Feedbacks and Desertification: The Mediterranean Model. J. Clim. 18, 684–701.

Niessen, F., Kelts, K., 1989. The deglaciation and Holocene sedimentary evolution of southern perialpine Lake Lugano—implications for Alpine paleoclimate. Eclogae Geol. Helv. 82 (1), 235–263.

Okuda, M., Yasuda, Y., Setoguchi, T., 2001. Middle to late Pleistocene vegetation history and climatic changes at Lake Kopais, Southeast Greece. Boreas 30, 73–82.

Oms, O., Garcés, M., Parés, J.M., Agustí, J., Anadón, P., Julià, R., 1994. Magnetostratigraphic characterization of a thick Lower Pleistocene lacustrine sequence from the Baza Basin (Betic Chain, Southern Spain). Phys. Earth Planet. Inter. 85, 173–180.

O'Neil, J.R., Clayton, R.N., Mayeda, T.K., 1969. Oxygen isotope fractionation between divalent metal carbonates. J. Chem. Phys. 51, 5547–5558.

Ortiz, J.E., 2000. Evolución paleoclimática durante el Pleistoceno de la mitad sur de la Península Ibérica mediante el estudio paleontológico y geoquímico de ostrácodos de la cuenca de Cúllar-Baza (Granada, España). PhD thesis, Politechnical University of Madrid, Spain. 563 pp.

Ortiz, J.E., Torres, T., Llamas, J.F., Canoira, L., García-Alonso, P., García de la Morena, M.A., Lucini, M., 2000. Dataciones de algunos yacimientos paleontológicos de la cuenca de Guadix-Baza (sector de Cúllar-Baza, Granada, España) y primera estimación de edad de la apertura de la cuenca mediante el método de racemización de aminoácidos. Geogaceta 28, 109–112.

Ortiz, J.E., Torres, T., Delgado, A., Julià, R., Llamas, F.J., Soler, V., Delgado, J., 2004a. Numerical dating algorithms of amino acid racemization ratios analyzed in continental ostracodes of the Iberian Peninsula (Spain). Application to Guadix-Baza Basin (southern Spain). Quat. Sci. Rev. 23 (5–6), 717–730.

Ortiz, J.E., Torres, T., Delgado, A., Julià, R., Lucini, M., Llamas, F.J., Reyes, E., Soler, V., Valle, M., 2004b. The palaeoenvironmental and palaeohydrological evolution of Padul Peat Bog (Granada, Spain) over one million years, from elemental, isotopic, and molecular organic geochemical proxies. Org. Geochem. 35 (11–12), 1243–1260.

Palacios-Fest, M.L.R., Cohen, A.S., Ruiz, J., Blank, B., 1993. Comparative paleoclimatic interpretations from nonmarine ostracodes using faunal assemblages, trace elements shell chemistry and stable isotope data. Climate change in continental isotopic records. Geophys. Monogr. 78, 179–189.

Palmqvist, P., Grokke, D.R., Arribas, A., Farina, R.A., 2003. Paleoecological reconstruction of a lower Pleistocene large mammal community using biogeochemical (delta C-13, delta N-15, delta O-18, Sr:Zn) and ecomorphological approaches. Paleobiology 29, 205–229.

Pate, J.S., 2001. Carbon isotope discrimitation and plant water-use efficiency: case scenarios for C3 plants. In: Unkovich, M., Pate, J., McNeill, A., Gibbs, D.J. (Eds.), Stable Isotope Techniques in the Study of Biological Processes and Funtioning of Ecosystems. Kluwer Scientific, Dordrecht, pp. 19–36.

Peña, J.A., 1985. La Depresión de Guadix-Baza. Est. Geol. 41, 33–46.

Petit, J.R., Jouzel, J., Raynaud, D., Barkov, N.I., Barnola, J.M., Basile, I., Bender, M., Chappellaz, J., Davis, J., Delaygue, G., Delmotte, M., Kotlyakov, V.M., Legrand, M., Lipenkov, V., Lorius, C., Pépin, L., Ritz, C., Saltzman, E., Stievenard, M., 1999. Climate and atmospheric history of the past 420,000 years from the Vostok ice core, Antarctica. Nature 399, 429–436.

Planas, M.D., 1973. Composición, ciclo y productividad del fitoplancton del lago de Banyoles. Oecol. Aquat. 1, 3–106.

Pons, A., Reille, M., 1988. The Holocene and upper Pleistocene pollen record from Padul (Granada, Spain): a new study. Palaeogeogr. Palaeoclimatol. Palaeoecol. 66, 243–263.

Reille, M., de Beaulieu, J.L., 1990. History of the Würm and Holocene vegetation in Western Velay (Massif Central, France): a comparison of pollen analysis from three corings at Lac du Bouchet. Rev. Paleobot. Palynol. 54, 233–248.

Ricketts, R.D., Johnson, T.C., Brown, E.T., Rasmussen, K.A., Romanovsky, V.V., 2001. The Holocene paleolimnology of Lake Issyk-Kul, Kyrgyzstan: trace element and stable isotope composition of ostracodes. Palaeogeogr. Palaeoclimatol. Palaeoecol. 176, 207–227.

Riesenfeld, E.H., Chang, T.L., 1936. Uber den Gehalt an HDO und $H_2^{18}O$ in Regen und Schnee. Berichte der Chem. Gesellschaft. Jahrg. 69, 1305–1307.

Roca, J.R., Wansard, G., 1997. Temperature influence on development and calcification of *Herpetocypris brevicaudata* Kaufmann, 1900 (Crustacea: Ostracoda) under experimental conditions. Hydrobiologia 347, 91–95.

Rogers, K.L., Larson, E.E., Smith, G., Katzman, D., Smith, G.R., Cerling, T., Wang, Y., Baker, R.G., Lohman, K.C., Repenning, C.A., Patterson, P., Mackie, G., 1992. Pliocene and Pleistocene geologic and climatic evolution in the San Luis Valley of south-central Colorado. Palaeogeogr. Palaeoclimatol. Palaeoecol. 94, 55–86.

Romanek, C.S., Grossman, E.L., Morse, J.W., 1992. Carbon isotopic fractionation in synthetic aragonite and calcite: effects of temperature and precipitation rate. Geochim. Cosmochim. Acta 56, 419–430.

Rosen, M.R., 1994. The importance of groundwater in playas: a review of playa classifications and the sedimentology and hydrology of playas. In: Rosen, M.R. (Ed.), Paleoclimate and Basin Evolution of Playa Systems. Geol. Soc. Amer., Spec. Pap., vol. 289, pp. 1–8.

Rozanski, K., Araguas-Araguas, L., Gonfiatini, R., 1993. Isotopic patterns in modern global precipitation. In: Smart, P.K., Lohmann, K.C., Mckenzie, J., Savin, S. (Eds.), Climate Change in Continental Isotopic Records. American Geophysical Union Geophysical Monograph, vol. 78, pp. 1–36.

Sage, R.F., 2004. The evolution of C4 photosynthesis. New Phytol. 161, 341–370.

Schwalb, A., Dean, W.E., 2002. Reconstruction of hydrological changes and response to effective moisture variations from North-Central USA lake sediments. Quat. Sci. Rev. 21, 1541–1554.

Schwalb, A., Burns, S.B., Kelts, K., 1999. Holocene environments from stable isotope stratigraphy of ostracods and authigenic carbonate in Chilean Altiplano Lakes. Palaeogeogr. Palaeoclimatol. Palaeoecol. 148, 153–168.

Schwarcz, H.P., Eyles, N., 1991. Laurentide ice sheet inferred from stable isotopic composition (O, C) of ostracodes at Toronto, Canada. Quat. Res. 35, 305–320.

Shackleton, N.J., 1995. New data on the evolution of Pliocene climatic variability. In: Vrba, E.S., Denton, G.H., Partidge, T.C., Burckle, L. H. (Eds.), Palaeoclimate and Evolution with Emphasis on Human Origins. Yale University Press, New Haven, pp. 242–248.

Smith, G.I., Bischoff, J.L., 1997. An 800,000-year paleoclimatic record from Core OL-92, Owens Lake, southeast California. Geol. Soc. Am., Spec. Paper 317 (165 pp.).

Sohn, I.G., 1958. Chemical constituents of ostracodes: some applications to paleontology and paleoecology. J. Paleontol. 32, 730–736.

Soria, J.M., 1993. La sedimentación neógena entre sierra Arana y el río Guadiana Menor (Cordillera Bética Central). Evolución desde un margen continental hasta una cuenca intramontañosa. PhD thesis, Universidad de Granada, 292 pp.

Soria, J.M., 1996. Historia de la subsidencia y levantamiento en el margen norte de la cuenca intramontañosa de Guadix (Cordillera Bética central). Geogaceta 20 (2), 464–467.

Spiro, B., Gibson, P.J., Shaw, H.F., 1993. Eogenetic siderites in lacustrine oil shales from Queensland, Australia, a stable isotope study. Chem. Geol. 106, 415–427.

Steig, E.J., Morse, D.L., Waddington, E.D., Stuiver, M., Grootes, P. M., Mayewski, P.M., Whitlow, S.I., Twickler, M.S., 2000. Wisconsinan and Holocene climate history from an ice core at Taylor Dome, western Ross Embayment, Antarctica. Geogr. Ann. 82A, 213–235.

Stiller, M., Rounick, J.S., Shasha, S., 1985. Extreme carbon-isotope enrichments in evaporite brines. Nature 316, 434–435.

Swart, P.K., Burns, S.J., Leder, J.J., 1991. Fractionation of the stable isotopes of oxygen and carbon in carbon dioxide during the reaction of calcite with phosphoric acid as a function of temperature and technique. Chem. Geol. 86, 89–96.

Talbot, M.R., 1990. A review of the palaeohydrological interpretation of carbon and oxygen isotopic ratios in primary lacustrine carbonates. Chem. Geol. 80, 261–279.

Teeri, J.A., Stowe, L.G., 1976. Climatic patterns and the distribution of C4 grasses in North America. Oecologia 23, 1–12.

Torres, T., Llamas, J., Canoira, L., García-Alonso, P., García-Cortés, A., Mansilla, H., 1997. Amino acid chronology of the Lower Pleistocene deposits of Venta Micena (Orce, Granada, Andalusia, Spain). Org. Geochem. 26, 85–97.

Torres, T., Ortiz, J.E., Soler, V., Reyes, E., Delgado, A., Valle, M., Cobo, R., Julià, R., Badal, E., García de la Morena, M.A., García-Martínez, M.J., Fernández-Gianotti, J., Calvo, J.P., Cortés, A., 2003a. Pleistocene lacustrine basin of the east domain of Guadix-Baza Basin (Granada, Spain): sedimentology, chronostratigraphy and palaeoenvironment. In: Valero-Garcés, B. (Ed.), Limnogeología en España: un tributo a Kerry Kelts. Consejo Superior de Investigaciones Científicas, Madrid, pp. 151–185.

Torres, T., Ortiz, J.E., Alcalde, C., Badal, E., Castroviejo, R., Cobo, R., Chacón, E., Delgado, A., Demoustier, A., Fernández-Gianotti, J., Figueiral, I., García-Amorena, I., García-Martínez, M.J., Llamas, J. F., Julià, R., Postigo, J.M., Rubiales, J.M., Reyes, E., Sepherd, T., Soler, V., Valle, M., 2003b. Evolución paleoambiental de la mitad sur de la Península Ibérica. Aplicación a la evaluación del comportamiento de los repositorios de residuos radiactivos. Publicación Técnica, vol. 04. ENRESA. 173 pp.

Turpen, J., Angell, R., 1971. Aspects of molting and calcification in the ostracode *Heterocypris*. Biol. Bull. 140, 331–338.

Tzedakis, P.C., 1993. Tree populations in northwest Greece through multiple Quaternary climatic cycles. Nature 364, 437–440.

Tzedakis, P.C., 1994. Vegetation change through glacial–interglacial cycles: a long pollen sequence perspective. Philos. Trans. R. Soc. Lond., B 345, 403–432.

Tzedakis, P.C., McManus, J.F., Hooghiemstra, H., Oppo, D.W., Wijmstra, T.A., 2003. Comparison of changes in vegetation in northeast Greece with records of climate variability on orbital and suborbital frequencies over the last 450,000years. Earth Planet. Sci. Lett. 212, 197–212.

Valero-Garcés, B.L., Zeroual, E., Kelts, K., 1998. Arid phases in the western Mediterranean region during the Last Glacial Cycle reconstructed from lacustrine records. In: Benito, G., Baker, V.R., Gragory, K.J. (Eds.), Paleohydrology and Environmental Change. Wiley, London, pp. 67–80.

Valero-Garcés, B.L., Gonzáez-Saméniz, P., Degado-Huertas, A., Navas, A., Machín, J., Kelts, K., 2000. Lateglacial and Late Holocene environmental and vegetational change in Salada Mediana, central Ebro Basin, Spain. Quat. Int. 73/74, 29–46.

Valero-Garcés, B.L., González-Sampériz, P., Navas, A., Machin, J., Mata, P., Delgado-Huerta, A., Bao, R., Moreno-Caballud, A., Carrión, J.S., Schwalb, A., González-Barrios, A., 2006. Human Impact since Medieval times and Recent Ecological Restoration in a Mediterranean Lake: The Laguna Zoñar (Spain). J. Paleolimnol. 441–465.

Vera, J.A., 1970. Estudio estratigráfico de la Depresión de Guadix-Baza. Bol. Instituto Geomin. Esp. 81, 429–462.

Viseras, C., Fernández, J., 1992. Sedimentary basin destruction inferred from the evolution of drainage systems in the Betic Cordillera, southern Spain. J. Geol. Soc. (Lond.) 149, 1021–1029.

von Grafenstein, U., Erlenkeuser, H., Müller, J., Kleinmann-Eisenmann, A., 1992. Oxygen isotope records of benthic ostracods in Bavarian lake sediments. reconstruction of late and post glacial air temperatures. Naturwissenschaften 79, 145–152.

von Grafenstein, U., Erlernkeuser, H., Trimborn, P., 1999. Oxygen and carbon isotopes in modern fresh-water ostracod valves: assessing vital offsets and autecological effects of interest for palaeoclimate studies. Palaeogeogr. Palaeoclimatol. Palaeoecol. 148, 133–152.

Wansard, G., De Deckker, P., Juliá, R., 1998. Variability in ostracod partition coefficients D(Sr) and D(Mg) implications for lacustrine palaeoenvironmental reconstructions. Chem. Geol. 146, 39–54.

Whittaker, A., Cope, J.W.C., Cowie, J.W., Gibbons, W., Hailwood, E., House, M.R., Jenkins, G.D., Rawson, P.F., Rushton, A.W.A., Smith, D.G., Thomas, A.T., Wimbledon, W.A., 1991. A guide to stratigraphical procedure. J. Geol. Soc. (Lond.) 148, 813–824.

Wijmstra, T.A., 1969. Palynology of the first 30m of a 120m deep section in Northern Greece. Acta Bot. Neer. 18, 511–527.

Wijmstra, T.A., Smit, A., 1976. Palynology of the middle part (30–78m) of the 120m deep section in northern Greece (Macedonia). Acta Bot. Neer. 25, 297–312.

Winograd, I.J., Coplen, T.B., Landwehr, J.M., Riggs, A.C., Ludwig, K. R., Szabo, B.J., Kolesar, P.T., Revesz, K.M., 1992. Continuous 500,000-year climate record from vein calcite in Devils Hole, Nevada. Science 258, 255–260.

Winograd, I.J., Landwehr, J.M., Ludwig, K.R., Coplen, T.B., Riggs, A. C., 1997. Duration and structure of the past four interglaciations. Quat. Res. 48, 141–154.

Woillard, G., 1978. Grande pile peat bog: a continuous pollen record for the last 140,000years. Quat. Res. 9, 1–21.

Xia, J., Ito, E., Engstrom, D.R., 1997. Geochemistry of ostracode calcite: Part 1. An experimental determination of oxygen isotope fractionation. Geochim. Cosmochim. Acta 61 (2), 377–382.

Zanchetta, G., Bonadonna, F., Leone, G., 1999. A 37-meter record of paleoclimatological events from stable isotope data on continental molluscs in Valle di Castiglione, near Rome, Italy. Quat. Res. 52, 293–299.